Title: Parenteral nanoemulsions as promising carriers for brain delivery of risperidone: design, characterization and *in vivo* pharmacokinetic evaluation

Author: Sanela M. Đorđević Nebojša D. Cekić Miroslav M. Savić Tanja M. Isailović Danijela V. Randelović Bojan D. Marković Saša R. Savić Tamara Timić Stamenić Rolf Daniels Snežana D. Savić

PII: S0378-5173(15)30026-0
DOI: http://dx.doi.org/doi:10.1016/j.ijpharm.2015.07.007
Reference: IJP 15007

To appear in: *International Journal of Pharmaceutics*

Received date: 5-6-2015
Revised date: 1-7-2015
Accepted date: 2-7-2015

Please cite this article as: *Dstroke*or*DF*ević, Sanela M., Cekić, Nebojša D., Savić, Miroslav M., Isailović, Tanja M., Ran*DF*elović, Danijela V., Marković, Bojan D., Savić, Saša R., Stamenić, Tamara Timić, Daniels, Rolf, Savić, Snežana D., Parenteral nanoemulsions as promising carriers for brain delivery of risperidone: design, characterization and in vivo pharmacokinetic evaluation.International Journal of Pharmaceutics http://dx.doi.org/10.1016/j.ijpharm.2015.07.007

Parenteral nanoemulsions as promising carriers for brain delivery of risperidone: design, characterization and *in vivo* pharmacokinetic evaluation

Sanela M. Đorđević[a], Nebojša D. Cekić[b,c], Miroslav M. Savić[d], Tanja M. Isailović[a], Danijela V. Ranđelović[e], Bojan D. Marković[f], Saša R. Savić[b], Tamara Timić Stamenić[d], Rolf Daniels[g], Snežana D. Savić[a]*

[a]Department of Pharmaceutical Technology and Cosmetology, Faculty of Pharmacy, University of Belgrade, Belgrade 11221, Serbia

[b]Faculty of Technology, University of Niš, Leskovac 16000, Serbia

[c]DCP Hemigal, Leskovac 16000, Serbia

[d]Department of Pharmacology, Faculty of Pharmacy, University of Belgrade, Belgrade 11221, Serbia

[e]ICTM – Institute of Microelectronic Technologies, University of Belgrade, Belgrade 11000, Serbia

[f]Department of Pharmaceutical Chemistry, Faculty of Pharmacy, University of Belgrade, Belgrade 11221, Serbia

[g]Institut für Pharmazeutische Technologie, Eberhard-Karls Universität Tübingen, Tübingen, Germany

*Corresponding author: Dr Snežana D. Savić, Department of Pharmaceutical Technology and Cosmetology, Faculty of Pharmacy, University of Belgrade, Vojvode Stepe 450, 11221 Belgrade, Serbia

Tel.: +381-11-3951366; Fax: +381-11-3972840

E-mail address: snexs@pharmacy.bg.ac.rs (S. D. Savić)

Graphical abstract

Abstract

This paper describes design and evaluation of parenteral lecithin-based nanoemulsions intended for brain delivery of risperidone, a poorly water-soluble psychopharmacological drug. The nanoemulsions were prepared through cold/hot high pressure homogenization and characterized regarding droplet size, polydispersity, surface charge, morphology, drug–vehicle interactions, and physical stability. To estimate the simultaneous influence of nanoemulsion formulation and preparation parameters – co-emulsifier type, aqueous phase type, homogenization temperature – on the critical quality attributes of developed nanoemulsions, a general factorial experimental design was applied. From the established design space and stability data, promising risperidone-loaded nanoemulsions (mean size about 160 nm, size distribution < 0.15, zeta potential around –50 mV), containing sodium oleate in the aqueous phase and polysorbate 80, poloxamer 188 or Solutol® HS15 as co-emulsifier, were produced by hot homogenization and their ability to improve risperidone delivery to the brain was assessed in rats. Pharmacokinetic study demonstrated erratic brain profiles of risperidone following intraperitoneal administration in selected nanoemulsions, most probably due to their different droplet surface properties (different composition of the stabilizing layer). Namely, polysorbate 80-costabilized nanoemulsion showed increased (1.4–7.4-fold higher) risperidone brain availability compared to other nanoemulsions and drug solution, suggesting this nanoemulsion as a promising carrier worth exploring further for brain targeting.

Keywords: parenteral nanoemulsions; brain targeting; poorly water-soluble drugs; general factorial design; physical stability; pharmacokinetics.

1. Introduction

Despite the progress achieved in development of modern strategies for brain targeting, effective treatment of central nervous system (CNS) disorders still remains a complicated and challenging task due to the presence of a restrictive blood-brain barrier (BBB) which is a major obstacle to the delivery of drugs directly to the brain (Shinde et al., 2011; Wong et al., 2012). Among the reported nanotechnological strategies, an increasing attention has been recently focused on nanoemulsions as potential carriers for CNS therapeutics, due to their attractive advantages including uniform and very small droplet size, high solubilization capacity for lipophilic drugs, good tolerability and greater bypass of the reticulo-endothelial system (RES). Additionally, an improved penetration through biological barriers, possibly enhanced bioavailability, controlled drug release and organ targeting could be expected with these systems (Shinde et al., 2011; Benita and Levy, 1993; Constantinides et al., 2008). While lipid nanoemulsions have been traditionally employed for parenteral nutrition and to solubilize and intravenously (i.v.) deliver lipophilic drugs (Li et al., 2011; Constantinides et al., 2008), only few reports on the nanoemulsions as carriers for parenteral delivery of drugs to the brain have been published up to now (Madhusudhan et al., 2007; Prabhakar et al., 2013; Đorđević et al., 2013).

The present paper was aimed at formulating parenteral nanoemulsions as brain drug targeting systems and evaluating their ability to improve the brain uptake of the incorporated drug, starting from analysis of the physicochemical properties of developed nanoemulsions and assessing their relationships with potential for brain drug delivery. For this purpose, placebo and drug-loaded nanoemulsions were designed with the aid of experimental design, prepared by high pressure homogenization (HPH) and characterized for their droplet size, size distribution, surface charge, viscosity, morphology, drug–vehicle interactions and stability.

Risperidone (RSP), a poorly water-soluble "atypical" antipsychotic drug, was chosen as a model compound to be incorporated into nanoemulsion droplets. Commercially available dosage forms of RSP (conventional and orally disintegrating tablet, oral solution and long-acting intramuscular injection) have certain drawbacks, such as swallowing problems or slow onset of the effect in acute psychosis or emergency situations (D'Souza et al., 2013; Rund et al., 2006). Although several attempts have been made to formulate various drug delivery systems of RSP – microemulsions (Kumar et al., 2008), polymeric nanoparticles (Muthu et al., 2009), solid lipid nanoparticles (Silva et al., 2012), polymeric micelles (Ould–Ouali et al., 2005), polymeric microspheres (D'Souza et al., 2013), in situ forming matrix depot (Lin et al., 2011) – no studies have been reported on enhancing the brain permeability of RSP using parenteral nanoemulsions as drug carriers. For these reasons, the development of nanoemulsions intended for delivery of RSP to the brain after parenteral administration was of particular interest to this investigation.

Various formulation factors (type and concentration of oils and emulsifiers), preparation conditions (homogenization temperature, pressure and number of cycles) as well as the way of drug incorporation in the inner phase of the nanoemulsion may profoundly affect its physicochemical properties and stability, and consequently, the *in vivo* pharmacokinetic behavior and efficacy (Benita and Levy, 1993; Nordén et al., 2001; Jumaa and Müller, 2002; Đorđević et al., 2013). Hence, it is highly desirable to have a good understanding and control of these complex parameters. Design of experiments approach has been recognized as a useful tool for development, improvement and optimization of nanoemulsion formulation and preparation, and a couple of studies using this methodology have been investigating the influence of formulation and/or processing variables on nanoemulsion properties and stability (Kelmann et al., 2007; Đorđević et al., 2013; Marín-Quintero et al., 2013). In this vein, the one objective of the present paper was to apply a general factorial design for identification of

the significant main and interaction effects of experimental factors (co-emulsifier type, aqueous phase type and homogenization temperature) in order to find optimal conditions leading to the nanoemulsions with desired physicochemical features.

Bearing in mind that nanoemulsion system on its own may affect the pharmacokinetic behavior of incorporated drug, and consequently its therapeutic effect (Hanefeld et al., 2012), the plasma and brain pharmacokinetics of RSP were studied after intraperitoneal (i.p.) administration of a series of nanoemulsions in rats. We wanted to know whether nanoemulsion composition, particularly co-emulsifier type, affects RSP pharmacokinetics, including brain targeting efficiency, after administration of selected RSP-loaded nanoemulsions via parenteral route. To the best of our knowledge, this is the first study conducted on formulation of RSP into parenteral nanoemulsion and on investigation of the influence of nanoemulsion formulation, on its own, on the delivery of RSP to the brain. As a result, this study could shed light on the parenteral nanoemulsions in the context of their further exploitation as carriers for brain drug delivery.

2. Materials and methods

2.1. Materials

RSP was kindly donated by Zdravlje Actavis (Leskovac, Serbia). Medium chain triglycerides (MCT) were purchased from Fagron GmbH & KG (Barsbüttel, Germany). Soybean oil (Lipoid Purified Soybean Oil 700), soybean lecithin (Lipoid S 75) and sodium oleate (Lipoid Sodium Oleate B) were generously gifted by Lipoid GmbH (Ludwigshafen, Germany). Kolliphor® P 188 (poloxamer 188, PL188) and Kolliphor® HS 15 (polyoxyl/macrogol 15 hydroxystearate, Solutol® HS 15, SHS15) were kindly supplied by BASF SE (Ludwigshafen,

Germany). Polysorbate 80 (P80, polyoxyethylensorbitan monooleate), benzyl alcohol and butylhydroxytoluene (BHT) were obtained from Sigma-Aldrich Co. (St. Louis, MO, USA), while glycerol was provided by Merck KGaA (Darmstandt, Germany). Sodium hydroxide and potassium phosphate monobasic were purchased from Sigma-Aldrich Chemie GmbH (Steinheim, Germany). Water used in the preparation of formulations was double-distilled, whereas ultra-pure water, used in analyses, was obtained with a GenPure apparatus (TKA Wasseranfbereitungssysteme GmbH, Neiderelbert, Germany). All other chemicals and reagents used were of pharmaceutical or HPLC grade and used as received without further purification.

2.2. Solubility study

The solubility of RSP in pure oils (MCT and soybean oil), mixtures of oils (MCT–soybean oil at ratios 2:1 and 4:1, w/w) and in oil phases containing 2% (w/w) of soybean lecithin was determined by shake flask method (for details see Supplementary material).

2.3. Preparation of nanoemulsions

All nanoemulsions were prepared by cold (25 ºC) or hot (50 ºC) HPH according to the recently published, but slightly modified procedure (Đorđević et al., 2013). Firstly, the oil and the aqueous phases were separately prepared. The oil phase, consisting of 20% (w/w) of oil (a mixture of MCT and soybean oil at a mass ratio of 4:1), 2% (w/w) of lipophilic emulsifier (soybean lecithin) and 0.05% (w/w) of antioxidant (BHT), was heated at 70 ºC under slight magnetic stirring, until lecithin was completely dissolved. The obtained oil phase was then allowed to cool down to the desired production temperature (25 ºC or 50 ºC) and,

afterward, benzyl alcohol (2%, w/w) was added. The aqueous phase was prepared by dissolving 2% (w/w) of hydrophilic emulsifier (P80, PL188 or SHS15) in 0.01 M phosphate buffer solution (PBS) (pH 9) or in double-distilled water containing 0.03% (w/w) sodium oleate (SOS) (pH 9). To adjust isotonicity, glycerol (2.25%, w/w) was added to the aqueous phase, which was kept at 25 ºC or heated to 50 ºC.

The phases were combined by adding the aqueous phase to the oil phase, both being kept at the same temperature, and further pre-homogenized with a rotor-stator homogenizer (IKA Ultra-Turrax® T25 digital, IKA®-Werke GmbH & Co. KG, Staufen, Germany) at 10000 rpm for 3 min. The obtained coarse emulsion was subsequently homogenized with a high-pressure homogenizer (EmulsiFlex-C3, Avestin Inc., Ottawa, Canada) at 500 bar for 10 repeated cycles. The resulting nanoemulsion was divided into two parts that were subjected to aseptic filtration through 0.22 μm membrane filter or to thermal sterilization in Autoclave Series 250 (Sutjeska, Belgrade, Serbia) at 121 °C for 15 min. When RSP was incorporated into the nanoemulsion, it was dissolved in benzyl alcohol as a co-solvent, and prepared solution (50 mg/g) was added to the oil phase to obtain a final drug concentration of 1 mg/g. All formulations were stored in crimped glass vials at 25 ºC and one day after preparation, their characterization was performed. All measurements were done in triplicate.

2.4. Factorial design study

During the nanoemulsion development, a computer generated general factorial experimental design was employed to identify and estimate the effects and interactions of multiple formulation and preparation factors and to establish their relationships with critical quality attributes of developed nanoemulsions. Preliminary experiments were conducted and it was determined that the type of co-emulsifier and the type of aqueous phase are important

formulation variables that can significantly affect the physicochemical properties and stability of nanoemulsions. On the other hand, the temperature of homogenization process was established to be the critical process variable which influences droplet size reduction via HPH. Based on these findings, the three independent variables selected for the factorial analysis and their respective levels were: the co-emulsifier type (A) – P80/PL188/SHS15; the aqueous phase type (B) – PBS/SOS; and the HPH method (C) – cold/hot (Table 1). The droplet size (Z-Ave), polydispersity index (PDI), and zeta potential (ZP) of nanoemulsions were set as the response variables.

According to the applied general factorial design, a total of 24 experimental runs, including 2 replicates per batch, were generated and randomly performed. The factorial design matrix and the responses of each experiment are given in Table 1 and Table S1 (Supplementary material), respectively. The general form of factorial model chosen to fit the experimental data can be found in Supplementary material. For building design, data processing and statistical analysis, the Design-Expert® software v. 9.0.1 trial (Stat-Ease Inc., Minneapolis, Minnesota, USA) was employed. The best polynomial models for analysis of nanoemulsions were proposed based on significant model terms ($p < 0.05$), insignificant lack of fit, multiple correlation coefficient (R^2), and adjusted multiple correlation coefficient (adjusted R^2) provided by Design-Expert®. Interaction plots and three-dimensional response surface plots displaying evaluated responses (Z-Ave, PDI, ZP) at different factor level combinations were also constructed.

2.5. Nanoemulsion characterization

2.5.1. Droplet size and size distribution analysis

The mean droplet size (intensity weighted mean diameter, Z-average diameter, Z-Ave) and droplet size distribution (PDI) of the nanoemulsions were determined by photon correlation spectroscopy (PCS), using a Zetasizer Nano ZS90 (Malvern Instruments Ltd., Worcestershire, UK). Before measurement, each nanoemulsion sample was diluted with ultra-pure water or freshly prepared 0.01 M PBS (1:500, v/v). The measurements were performed at 25 ºC at a fixed scattering angle of 90º using a He-Ne laser at 633 nm.

To detect a small fraction of larger emulsion droplets, laser diffractometry (LD) was applied as additional method for particle sizing. LD was performed using a Malvern Mastersizer 2000 (Malvern Instruments Ltd., Worcestershire, UK) and the volume weighted diameters d(0.5), d(0.9) and D[4,3] were calculated as critical parameters of this part of nanoemulsion characterization.

2.5.2. Zeta potential analysis

The droplet surface charge of the nanoemulsions was determined using a Zetasizer Nano ZS90 (Malvern Instruments Ltd., Worcestershire, UK) by measuring the electrophoretic mobility of nanoemulsion droplets, which was converted to the ZP using in-built software. The measurements were performed at 25 ºC immediately upon appropriate dilution of samples (1:500, v/v) with the electrolyte solution consisted of ultra-pure water with constant conductivity (about 50 μS/cm) adjusted by 0.1 M PBS solution.

2.5.3. Viscosity measurements

Rheological behavior of selected blank and drug-loaded nanoemulsions was evaluated using a Visco Elite-R rotational viscometer (Fungilab S.A., Barcelona, Spain) equipped with the

low viscosity adapter (LCP) and controlled by Supervisc software (Fungilab S.A.). The measurements were performed at 20 ºC within the speed range 100–200 rpm.

2.5.4. Electrical conductivity measurements

The electrical conductivity of all samples was determined using a sensION^{TM} + EC71 conductivity meter (ShangHai Shilu Instruments Co., Ltd., Shanghai, China). The measurements were performed at 25 ºC by direct immersion of electrode into the sample.

2.5.5. pH value measurements

The pH values of all nanoemulsions were determined using a HI9321 pH meter (Hanna Instruments Inc., Michigan, USA). The measurements were performed at 25 ºC by direct immersion of pH meter glass electrode into samples.

2.5.6. Atomic force microscopy

To confirm the size measurements results and to visualize the morphology of the oil droplets in the nanoemulsions, atomic force microscopy (AFM) was employed using NTEGRA prima atomic force microscope (NT-MDT, Moscow, Russia). A drop (10 μL) of diluted nanoemulsion sample (1:100, v/v in ultra-pure water) was directly deposited onto circular mica substrate (Highest Grade V1 AFM Mica Discs, Ted Pella Inc., Redding, California, USA) and dried in vacuum to remove excess water. Measurements were carried out with the AFM operating in an intermittent-contact mode in air. NT-MDT NSGO1 silicon, N-type, Antimony doped, with Au reflective coating, cantilevers were used with the following

parameters: nominal force constant 5.1 N/m, resonance frequency 87–230 kHz, driving frequency 150 kHz, and the line scanning frequency 0.5 Hz. Post-acquisition processing of the obtained topography and "error signal" images was performed using the software Image Analysis 2.2.0 (NT-MDT, Moscow, Russia).

2.5.7. Differential scanning calorimetry

To evaluate the physical state of RSP in formulated nanoemulsions and possible interactions between drug and other components, the differential scanning calorimetry (DSC) was performed. The DSC thermograms of individual nanoemulsion components, RSP-loaded and RSP-free nanoemulsions were recorded using a Mettler DSC 820 apparatus (Mettler Toledo GmbH Analytical, Giessen, Germany). The nanoemulsion samples were prepared by placing a 10 µL of the nanoemulsion into standard aluminum pan and air dried. The dried samples were then accurately weighed, hermetically sealed, and scanned between 25 ºC and 250 ºC at a heating rate of 10 ºC/min under constant nitrogen flow. An empty aluminum pan was used as a reference. Thermoanalytical parameters were calculated using the Mettler Toledo STAR^e software.

2.5.8. Fourier transform infrared spectroscopy

To investigate any chemical interaction among incorporated drug and other ingredients, the Fourier transform infrared (FTIR) spectroscopy was also conducted. The FTIR spectra of pure nanoemulsion components, RSP-loaded and blank nanoemulsions were obtained using a BOMEM Hartmann & Braun MB-Series FTIR spectrophotometer (ABB Bomem Inc., Quebec, Canada). The samples were prepared as described previously (Đorđević et al., 2013)

and recorded between 4000 and 400 cm^{-1}, using 10 scans for each spectrum, with a resolution of 4 cm^{-1}.

2.5.9. Stability study

To evaluate the physical stability of developed nanoemulsions, all formulations were stored at room temperature for four months. The mean droplet size, PDI, ZP, viscosity, pH, and electrical conductivity of the nanoemulsions were determined using the previously described techniques. Statistical analysis of differences in measured parameters (one day after production and after four months of storage or after autoclaving) was performed using Student's *t*-test. The p value of 0.05 was taken as the level of significance.

2.6. *In vivo* pharmacokinetic study

2.6.1. Experimental procedure and sample collection

Pharmacokinetic properties of developed RSP-loaded nanoemulsions and RSP solution (1 mg/mL RSP dissolved in double distilled water containing 0.25% (w/v) sodium chloride, 0.4% (w/v) tartaric acid and sufficient sodium hydroxide to adjust the pH to 5.0), were assessed in male *Wistar* rats (Military Farm, Belgrade, Serbia). The protocol for animal experiments conformed to EU Directive 2010/63/EU and was approved by the Ethical Committee on Animal Experimentation of the Faculty of Pharmacy, University of Belgrade, Serbia. The rats (250–300 g) were housed in plastic cages, 4 animals per cage, on a 12 h light/dark period (light on at 06:00 h), under controlled conditions of temperature (22 ± 1 °C),

relative humidity (40–70%) and illumination (120 lx). All animals were provided with pellet food and tap water *ad libitum*.

On the day of experiment, rats were randomly divided into 6 groups, each containing 18 animals (3 animals per each of 6 time points). The samples (RSP solution and four RSP-loaded nanoemulsions – RSP-P80Sh, RSP-PL188Sh, RSP-SHS15Sh, and RSP-LS75Sh) were administered i.p. in overnight fasted animals, at a single RSP dose of 1 mg/kg, corresponding to an injected volume of 1 mL/kg. In addition, to determine the absolute bioavailability, one group of rats received 1 mg/kg RSP solution by i.v. injection into the tail vein. At predetermined time intervals, i.e., 5, 10, 20, 40, 60, and 180 min after dosing, the blood samples of rats anesthetized with ketamine (100 mg/kg, i.p.) were collected in heparinized syringes via cardiac puncture and centrifuged (2500 rpm, 10 min) to obtain plasma. Thereafter, the rat was decapitated and intact brain was carefully removed from the skull, weighed, homogenized in 5 mL of methanol (IKA Ultra-Turrax® T25 digital), and homogenates were centrifuged at 6000 rpm for 20 min (Centrifuge MPW-56, MPW Med. Instruments, Warszawa, Poland).

2.6.2. Determination of risperidone concentration in rat plasma and brain tissue

To determine the concentration of RSP in plasma and supernatants of brain tissue homogenates, RSP was extracted from these samples by solid phase extraction according to the previously reported procedure (Đorđević et al., 2013). Concentration of RSP in the resulting eluates were determined by ultra-high performance liquid chromatography-tandem mass spectrometry (UHPLC-MS/MS). Details are provided in Supplementary material.

2.6.3. Pharmacokinetic analysis

Non-compartmental pharmacokinetic analysis in plasma and brain after i.p. administration of RSP-loaded nanoemulsions and i.p. as well as i.v. administration of RSP solution was performed with PK Functions for Microsoft Excel software (Usansky, Desai and Tang-Liu, Department of Pharmacokinetics and Drug Metabolism, Allergan, Irvine, CA; http://www.boomer.org/pkin/soft.html). The following pharmacokinetic parameters were calculated: maximum concentration (C_{max}), time to reach maximum concentration (T_{max}), area under the concentration *versus* time curve from zero to last measurable time point ($AUC_{0–t}$), terminal elimination half-life ($t_{1/2}$), and clearance ($CL = Dose/AUC_{0–t}$).

The relative bioavailability (F_{rel}) and absolute bioavailability (F_{abs}) of RSP following i.p. administration in nanoemulsions were determined relative to the i.p. and i.v. solution, respectively using the formula: $F = AUC_{0–t,\ RSP\ nanoemulsion}/AUC_{0–t,\ RSP\ solution}$. The brain targeting potential of developed RSP-loaded nanoemulsions after i.p. administration was also evaluated using the parameters such as brain-to-plasma drug concentration ratio, brain-to-plasma partition coefficient ($K_p = AUC_{0\text{-}t,\ brain}/AUC_{0\text{-}t,\ plasma}$), and therapeutic availability ($TA = AUC_{0\text{-}t,\ brain,\ RSP\ nanoemulsion}/AUC_{0\text{-}t,\ brain,\ RSP\ solution}$). The values of these parameters greater than 1 indicated good brain targeting of the formulation.

2.7. Statistical analysis

The results of the *in vivo* studies are shown as mean parameter value ± standard error of the mean (SEM) of three independent experiments. Whenever applicable, statistical differences between multiple groups were determined by one-way ANOVA with *post hoc* analysis using Tukey's HSD test for pairwise comparisons between groups. When the assumptions of ANOVA were not met, i.e., the variances of the groups were not equal, and the data could not

be transformed, a nonparametric Kruskal–Wallis test (one-way ANOVA by ranks) was performed and, in the case of significant difference, the nonparametric Mann–Whitney *U* test was used for pairwise group comparisons. Statistical analyses were performed using PASW Statistics software package, version 18.0 (SPSS Inc., Chicago, USA). The level of significance was set at $p < 0.05$.

3. Results and discussion

3.1. Preparation and characterization of nanoemulsions

The solubility of the drug in the internal oil phase is an important factor to consider when designing nanoemulsions as carriers for lipophilic drugs (Benita and Levy, 1993). RSP is a poorly water-soluble drug and thus it is essential to incorporate it in the oil core of nanoemulsion in order to successfully exploit the nanoemulsion advantages in brain drug delivery. Hence, to select the optimal oil phase for the formulation of the nanoemulsions, RSP solubility in two oils commonly used in commercial parenteral lipid emulsions, namely MCT and soybean oil, as well as in their mixtures, was investigated. The solubility of RSP in tested oils and mixtures of oils was very low (≤ 2.2 mg/mL at 25 °C), suggesting inefficient drug loading in the nanoemulsion with a fixed amount (20%, w/w) of oil phase.

As the target concentration of 1 mg/g RSP in the nanoemulsion was unattainable, the efforts have been made to solve the problem of the poor RSP solubility. Firstly, lecithin was added as a solubilizer to the oil/mixture of oils and, secondly, temperature elevation method was applied. The addition of lecithin did not result in the dissolution of appreciable amounts of drug – solubility was about 2 mg/mL at 25 °C. Although drug dissolution in the oil phase containing lecithin was achieved by heating, drug precipitation was observed after cooling to

the room temperature. Finally, an oil-miscible co-solvent, benzyl alcohol, was introduced in the formulation, and by dissolving RSP in this co-solvent it was possible to obtain a 1 mg/g concentration of the active, without the formation of drug crystals in the nanoemulsion.

Regarding the oil phase selection, it has been reported that the mixture of MCT and long chain triglyceride (LCT) such as soybean oil can reduce the viscosity of LCT, nanoemulsion droplet size distribution as well as interfacial tension and, hence, might promote physical stability of nanoemulsions (Driscoll et al., 2000). Considering this and our experience with diazepam-loaded nanoemulsions (Đorđević et al., 2013), the mixture of MCT and soybean oil (4:1, w/w) was chosen as the oil phase for the formulation of unloaded and RSP-loaded nanoemulsions.

Based on previous experiments (Ma et al., 2013; Đorđević et al., 2013), the soybean lecithin was selected as the main emulsifier for nanoemulsion preparation in the present study. Furthermore, in order to improve the stability of nanoemulsions during storage and thermal sterilization, different types of co-emulsifiers, that form a close-packed, complex film with lecithin at the oil-water interface, were also employed. Selection of co-emulsifiers was carried out in accordance with their acceptability for parenteral administration and, more importantly, with our final goal – brain drug delivery. We selected P80, PL188 and SHS15, as promising functional excipients that have shown tendency to enhance brain uptake of drugs by acting as P-glycoprotein inhibitors, permeation enhancers, stealth agents or promoters of receptor-mediated endocytosis (Kreuter, 2001; Batrakova and Kabanov, 2008; Shinde et al., 2011; Kasongo et al., 2011).

To avoid pH alterations during storage and to keep RSP as a weak base in the oil phase, a 0.01 M PBS (pH 9) and double-distilled water containing sodium oleate (SOS) (pH 9) were used as the aqueous phases of the nanoemulsions. Besides the role of an auxiliary stabilizer of the phospholipid surface layer (Shi et al., 2009; Werling et al., 2008), sodium oleate also

served as a buffering agent to maintain the pH of prepared nanoemulsion formulations to a desirable value.

A total of 12 different unloaded nanoemulsion formulations were prepared using cold or hot HPH, concordant with applied experimental design (Table 1). The resulting nanoemulsions were highly fluid and homogenous with milky-white appearance. Representative nanoemulsion parameters (Z-Ave, PDI, ZP, pH and electrical conductivity) one day after preparation and after four months of storage at room temperature, as well as after autoclaving, are presented in Table S1 (see Supplementary material). The PCS particle size analysis (Table S1, Supplementary material) confirmed that the mean droplet size of all prepared unloaded nanoemulsions was in nanometer range (107–194 nm), with a relatively narrow particle size distribution (PDI < 0.15), suggesting that the developed nanoemulsions were suitable for parenteral application. In addition, all formulations revealed negative ZP values, ranged from –43 to –59 mV (Table S1, Supplementary material), implying a sufficiently high negative surface charge for droplet-droplet repulsion and thus an enhanced nanoemulsion stability.

3.2. Factorial design study

It has been proposed that nanoemulsion droplet size, ZP and surface properties are the key parameters affecting the BBB passage, with the surfactant/emulsifier composition playing the most important role in this regard (Müller and Göppert, 2007; Keck et al., 2013; Voigt et al., 2014). Based on prior reports (Blasi et al., 2013; Dhawan et al., 2011; Wohlfart et al., 2012), we specifically assumed that the small (below 200 nm) and homogenous droplet size, negative ZP and hydrophilic droplet surface are prerequisites for efficient brain targeting and utilized the experimental design strategy to uncover the influence factors for these

parameters. More precisely, with the purpose of gaining better perception of how nanoemulsion critical properties are affected by variations of nanoemulsion composition (aqueous phase and co-emulsifier type) and preparation conditions (homogenization temperature), general factorial experimental design was applied, that allowed to elucidate various interactions between independent variables tested, which are not possible to detect with the traditional one-factor-at-a-time method.

Table S1 (Supplementary material) shows the results of measured responses for all unloaded nanoemulsions that were part of the general factorial design to establish the combination of variables and their interactions yielding nanoemulsions with desirable properties for brain drug targeting. For each dependent variable (Z-Ave, PDI, and ZP), the effects corresponding to the investigated factors (co-emulsifier type, aqueous phase type, and HPH method) and interactions were calculated. Factors and interactions with $p < 0.05$ were considered significant. The terms with insignificant influence on estimated responses were excluded, except those required to maintain hierarchy, and thus the reduced factorial models for nanoemulsion droplet size, size distribution and surface charge were generated. The resulting final response equations in terms of coded factors are given below:

$$ZAve(nm) = 164.45 + 2.67A[1] + 6.31A[2] + 6.41B - 23.42C + 2.21A[1]B - 3.85A[2]B + 0.47A[1]C + 4.66A[2]C + 6.10BC - 0.30A[1]BC - 5.37A[2]BC \quad (1)$$

$$PDI = 0.1100 + 0.0077A[1] - 0.0045A[2] + 0.0065B - 0.0120C + 0.0086A[1]B - 0.0070A[2]B + 0.0078A[1]C + 0.0045A[2]C + 0.0024BC - 0.0083A[1]BC - 0.0031A[2]BC \quad (2)$$

$$ZP(mV) = -50.52 + 0.81A[1] + 0.76A[2] + 1.86B + 2.94C - 1.02A[1]B + 2.25A[2]B - 1.20BC \quad (3)$$

The ANOVA showed the generated models for Z-Ave, PDI and ZP to be highly significant ($p < 0.0001$ for model F values) with non-significant lack of fit ($p > 0.01$; could be calculated only for ZP). The fitted models had high R^2, adjusted R^2, and adequate precision values (Z-Ave: 0.9982, 0.9966, 76.229; PDI: 0.9280, 0.8620, 14.028; ZP: 0.9388, 0.9120, 18.78, respectively), indicating that three listed responses are well described by the proposed models.

Fig. 1a shows the Pareto plot for the mean droplet size (Z-Ave) of nanoemulsions. The smaller the p value or, in other words, the higher the magnitude of each coefficient, the higher is the respective effect on the response. Nanoemulsion droplet size was significantly affected by all factors under study ($p < 0.0001$) with the following order: HPH method (C) > aqueous phase type (B) > co-emulsifier type (A) (Fig. 1a). Moreover, the interactions between these factors (co-emulsifier type/aqueous phase type – AB; co-emulsifier type/HPH method – AC; aqueous phase type/HPH method – BC) were also found to influence the Z-Ave of nanoemulsions at a significant level ($p < 0.0001$), with the BC interaction having the most pronounced effect.

A negative sign for the coefficient of HPH method in Eq. (1) represented an antagonistic effect on Z-Ave, meaning that the droplet size of nanoemulsions made at 50 °C (hot HPH) was smaller compared to those prepared at 25 °C (cold HPH). This may mean that the higher energy input during homogenization by increasing the production temperature from 25 °C to 50 °C caused a decrease in viscosity as wall as in the interfacial tension, which is expected to facilitate the production of smaller nanoemulsion droplets (Floury et al., 2000). The type of aqueous phase revealed a positive influence on the Z-Ave of nanoemulsions (Eq. (1)): the smaller droplet size was found to correlate with PBS, while the aqueous phase containing sodium oleate (SOS) produced nanoemulsions with larger droplet sizes. The choice of co-

emulsifier showed a quite different trend of influence on Z-Ave (Table S1, Supplementary material). While SHS15 appeared to yield nanoemulsions with smaller droplets, the impact of the co-emulsifier type on the nanoemulsion droplet size could be better understood through interpreting the significant two-factor interactions.

When analyzing AB interaction (Fig. 2), it is apparent that at lower processing temperature (cold HPH), no difference in droplet size of nanoemulsions prepared with different co-emulsifiers (P80, PL188, and SHS15) was observed, when PBS was used as an aqueous phase. In case of nanoemulsions produced with SOS as the aqueous phase, the Z-Ave of nanoemulsions containing SHS15 as co-emulsifier was lower than that of nanoemulsions costabilized by P80 or PL188, which had similar droplet sizes. Furthermore, when SOS was used instead of PBS, the Z-Ave of P80- and PL188-costabilized nanoemulsions tended to slightly increase, whereas in case of SHS15-nanoemulsions a lower Z-Ave was obtained (Fig. 2). At higher homogenization temperature (hot HPH), using SOS instead of PBS as the aqueous phase resulted in the increase of Z-Ave for all nanoemulsions, regardless the co-emulsifier used (Fig. 2). When comparing the influence of coemulsifier type on Z-Ave of nanoemulsions prepared at 50 °C with PBS as the aqueous phase, it can be noticed that PL188 produced nanoemulsions with larger droplets, whereas lower size was obtained with P80 and SHS15. Conversely, when SOS was used as the aqueous phase, the Z-Ave obtained for P80- and PL188-nanoemulsions was comparable and greater than droplet size of SHS15-nanoemulsions. The same trends regarding nanoemulsion Z-Ave could be also observed by analyzing the effects of AC and BC interactions (Fig. 2).

To obtain information about the homogeneity of nanoemulsions droplet sizes and, hence, about the quality of prepared nanoemulsion samples, the droplet size distribution (PDI) and its dependence on the factors varied was assessed, and results obtained from the model fitting procedure are shown in Eq. (2) and Fig. 1b. The PDI of nanoemulsions was significantly

influenced by the individually tested variables as well as by their combined effects. The HPH method appeared to have an inverted but the greatest influence on PDI, imposing that a higher homogenization temperature produced nanoemulsions with more homogenous sizes (lower PDI). The type of co-emulsifier was also found to be critically important in variations of nanoemulsion PDI and, more importantly, to strongly interact with other two factors, namely aqueous phase type and HPH method – AB and AC interaction, respectively (Fig. 3). It could be noticed that in case of nanoemulsions containing PBS as aqueous phase, the type of co-emulsifier influenced the PDI of nanoemulsions following the trend of $PDI_{P80} < PDI_{PL188} < PDI_{SHS15}$ and $PDI_{P80} > PDI_{PL188} > PDI_{SHS15}$ for nanoemulsions prepared with cold and hot HPH method, respectively. Conversely, when SOS was employed as the aqueous phase, P80 seemed to yield nanoemulsions with the largest PDI, whereas nanoemulsions derived from PL188 showed the lowest PDI values ($PDI_{P80} > PDI_{SHS15} > PDI_{PL188}$), irrespective of applied production temperature (Fig. 3). Moreover, when SOS was used instead of PBS as aqueous phase at lower production temperature (cold HPH), a tendency of PDI increase was shown in P80-based nanoemulsions, contrary to the SHS15-based nanoemulsions where PDI tended to decrease, while no difference was observed in PDI of PL188-based nanoemulsions. On the other hand, use of SOS instead of PBS at higher homogenization temperature (hot HPH) resulted in more heterogeneous droplet sizes for P80- and SHS15-nanoemulsions, whereas the PDI of PL188-nanoemulsions was only negligibly decreased (Fig. 3). When PBS was used as the aqueous phase, an increase of homogenization temperature from 25 °C to 50 °C induced an increase in PDI for P80-based nanoemulsions, whereas the PDI of PL188- and SHS15-nanoemulsions decreased. The variation in production method was the most effective in changing the PDI of nanoemulsions with SHS15 as co-emulsifier. However, in case of SOS-nanoemulsions, variation in temperature from 25

°C to 50 °C resulted in reduction of PDI of all nanoemulsions, irrespective of co-emulsifier used (Fig. 3).

Considering the ZP, Fig. 1c reveals that all the studied factors were significant and also positive (Eq. (3)), imposing a linear decreasing effect on the ZP of nanoemulsions. In addition, significant interactions were identified between co-emulsifier type and aqueous phase type (AB) and between aqueous phase type and HPH method (BC), as presented in Fig. 4. Judging from the value of coefficients in Eq.(3), the HPH method had the largest influence on nanoemulsion ZP – more negative ZP values were obtained when cold homogenization process was performed as compared to hot HPH method. It could be due to the larger droplet size of nanoemulsions prepared at 25 °C and, consequently, the smaller total surface area available for adsorption of surfactant molecules compared to formulations made at 50 °C. As a result, at a given concentration of surfactants in the formulation, more surfactant molecules are expected to be adsorbed per unit area in case of larger droplets leading to greater negative charge and, hence, more negative ZP values (cf. Verna et al., 2009). The factors interactions shown in Fig. 4 supported the above findings. It is obvious that the ZP of all nanoemulsions prepared with either PBS or SOS as aqueous phase in combination with any of the three co-emulsifiers (P80, PL188 or SHS15) decreased when HPH method was changed from cold to hot, with reduction in ZP more pronounced in PBS nanoemulsions. Likewise, the lower ZP values were obtained for all nanoemulsions prepared with cold HPH when using SOS instead of PBS as aqueous phase. In case of hot HPH, the ZP of P80- and SHS15-based nanoemulsions increased (became more negative), whereas in PL188-based formulations decreased, when SOS was used instead of PBS (Fig. 4).

3.3. Stability study – unloaded nanoemulsions

The physical stability of all unloaded nanoemulsions prepared according to the design of experiments was investigated after 4 months of storage at 25 °C as well as after heat sterilization by autoclaving (121 °C, 15 min). Data generated from the stability study (Table S1, Supplementary material) showed that the droplet size, PDI, and ZP – the most representative parameters in the control of emulsion stability – stayed practically unchanged during 4 months of storage for almost all investigated non-autoclaved nanoemulsion samples. A significant increase in droplet size of about 40–50 nm ($p < 0.05$) was only found for nanoemulsions formulated with PBS as aqueous phase and SHS15 as coemulsifier, prepared by either cold or hot HPH, but no visible free oil or phase separation was seen on visual inspection.

In addition, results given in Table S1 (see Supplementary material) revealed that the physical stability of all nanoemulsions produced with PBS was significantly altered during autoclaving. For example, for P80-costabilized nanoemulsions containing PBS, the complete phase separation due to energy-induced coalescence of oil droplets was observed. Nanoemulsions costabilized by PL188 demonstrated significant changes ($p < 0.05$) in the stability parameters: increase in Z-Ave, decrease in PDI, and increase in absolute ZP. Also, in nanoemulsions with SHS15, significant reduction of Z-Ave and PDI was detected upon autoclaving, but the size increased significantly ($p < 0.05$) with time. In contrast to the formulations with PBS, all investigated nanoemulsions containing SOS, irrespective of co-emulsifier type or preparation method, remained unchanged upon autoclaving in terms of droplet size, PDI, and charge, and the parameter values were stable within 4 months of storage at 25 °C. Thus, the stability of nanoemulsions against heat-stress during autoclaving was possibly promoted by the presence of sodium oleate which, in addition to pH buffering, might increase the negative charge of the droplet surface layer, contributing to the nanoemulsion electrostatic stabilization (Werling et al., 2008).

Additional information about storage stability and heat sterilization stability of investigated nanoemulsions was derived from the changes in pH and electrical conductivity over the evaluated period. The pH of most nanoemulsion samples significantly decreased ($p < 0.05$, Table S1, Supplementary material) during storage and autoclaving, but the pH values were still between 7 and 8, reflecting physiological compatibility and suitability for parenteral application. Concerning the electrical conductivity, slight but significant increases or decreases ($p < 0.05$, Table S1, Supplementary material) as a function of time and autoclaving were observed, but correlation between the change of this parameter and nanoemulsion instability was absent.

In summary, the results of stability investigation confirmed that the factors influencing nanoemulsion stability were the type of aqueous phase and the type of co-emulsifier. Combining all the stability parameters, we can conclude that nanoemulsions containing sodium oleate in aqueous phase (SOS) were more robust and more stable than those with PBS and they were considered as promising carriers for parenteral drug delivery.

3.4. Risperidone-loaded nanoemulsions – characterization and stability evaluation

According to data on polymeric and solid lipid nanoparticles (Blasi et al., 2013; Dhawan et al., 2011; Martins et al., 2012), the nanoemulsions with droplet sizes in the range of 100–200 nm were expected to have prolonged blood circulation time and hence potential increase in time for which the droplets remain in contact with the BBB and can be endocytosed by the brain blood vessel endothelial cells (Kreuter, 2001; Kreuter, 2005). Generally, the nanoemulsions with mean droplet diameter smaller than 200 nm, narrow droplet size distribution (PDI < 0.15) and sufficiently high negative surface charge (about –50 mV) were obtained within the design space in our study. Since in terms of physicochemical parameters

all designed nanoemulsions were appropriate for brain drug delivery, the most suitable formulations for drug incorporation were selected as a function of the smallest droplet size, the lowest size distribution and the highest stability for at least 4 months of storage at 25° C as well as upon autoclaving. In addition, knowing that the particle surface chemistry may take precedence over the droplet size and surface charge in determining BBB passage (Voigt et al., 2014), the type of co-emulsifier was also considered as a relevant factor in the selection between the unloaded nanoemulsions.

Three most promising formulations prepared by hot HPH, differing in the co-emulsifier (P80, PL188 or SHS15) and containing SOS as aqueous phase, were loaded with RSP and their comprehensive evaluation was performed. Table S2, provided in the Supplementary material, displays the physicochemical characteristics of selected RSP-loaded (RSP-P80Sh, RSP-PL188Sh, RSP-SHS15Sh) compared to corresponding unloaded nanoemulsions (P80Sh, PL188Sh, SHS15Sh) 1 day after production and after 4 months of storage at 25 °C. The RSP-loaded nanoemulsions behaved almost identically with respect to mean droplet size (Z-Ave around 160 nm), size homogeneity (PDI in the range of 0.10–0.13) and surface charge (ZP values about –50 mV). Supplementary LD particle size analysis confirmed that the droplet diameters of these RSP-loaded nanoemulsions were in nanometer range (d(0.5) about 170 nm; d(0.9) around 200 nm) with no particles above 1 µm, proving their feasibility for parenteral administration and brain drug delivery. Furthermore, the pH values (8.2–8.4) and sufficiently low viscosity (6 to 11 mPa·s) additionally demonstrated the suitability of developed RSP-loaded nanoemulsions for parenteral use.

The comparison of drug-loaded with corresponding unloaded nanoemulsions revealed that the incorporation of RSP did not significantly alter the nanoemulsion droplet size, size distribution and surface charge, with one exception (see Table S2 in the Supplementary material): the mean size of the SHS15-based RSP-loaded nanoemulsion (RSP-SHS15Sh) was

slightly (about 10 nm), but significantly ($p < 0.05$), higher than that of corresponding plain formulation (SHS15Sh), suggesting that the RSP might have been localized predominantly in the oil core of the nanoemulsion. On the other hand, it could be noticed that RSP contributed significantly ($p < 0.05$) to higher pH, higher electrical conductivity, and lower viscosity of the nanoemulsions (Table S2, Supplementary material), which might be related to the putative presence of a portion of drug molecules in the oil/water interface of the loaded nanoemulsions. Concerning the storage stability, all RSP-loaded nanoemulsions were found to be stable after four months, with only minor variations in measured physicochemical parameters (see Table S2 in the Supplementary material).

3.5. Drug–vehicle interactions and nanoemulsion characterization by DSC, FTIR, and AFM

The effect of drug loading on thermal behavior and structural properties of developed nanoemulsions as well as potential interactions among ingredients were examined using DSC technique. To avoid water evaporation event (broad endothermic peak around 100 ºC) and its influence on the nanoemulsion thermograms analysis, the native nanoemulsion samples were air-dried before DSC measurements. Fig. 5a displays the DSC thermal curves obtained for selected blank and RSP-loaded nanoemulsions, as well as for pure RSP. The DSC thermogram of pure RSP showed a sharp endothermic peak at 171.67 ºC, corresponding to the melting of the drug. In the DSC curves of both, RSP-loaded and unloaded nanoemulsions, a broad asymmetric endothermic peak was observed around 190 ºC, most likely due to benzyl alcohol evaporation. However, for RSP-containing nanoemulsion, no melting peak of the drug was detected, suggesting that RSP was molecularly dispersed, i.e., dissolved in the oil phase of the nanoemulsion.

To complement the findings of the thermal analysis, the FTIR spectroscopy was employed as a supplementary technique to find out possible intermolecular interactions between the drug and other components in the developed nanoemulsion systems. Fig. 5b shows the FTIR spectra of selected RSP-loaded and corresponding blank nanoemulsion, as well as of pure RSP, MCT–soybean oil mixture (4:1, w/w), and soybean lecithin (full description of characteristic absorption bands is provided in Supplementary material). The FTIR profile of nanoemulsion loaded with RSP did not show specific peaks corresponding to the drug, i.e., the described RSP peaks disappeared or were hidden under the peaks of oils. Also, no new peaks or shifts could be detected in this spectrum when compared with the FTIR spectrum of blank nanoemulsion, confirming the absence of any chemical interaction of RSP with other nanoemulsion ingredients. These results were in line with those obtained by DSC, indicating that RSP was uniformly dispersed, without any intermolecular drug–vehicle interaction or any hints of possible drug recrystallization in the nanoemulsions.

As a further part of nanoemulsion characterization, AFM analysis was performed to complete information about droplet size, size distribution, morphology, and the possible aggregation process within the system. The AFM images – error signal, 2D and 3D topography, obtained for 2×2 μm^2 area of the selected RSP-loaded nanoemulsion sample (RSP-P80Sh) are illustrated in Figs. 6a, 6b, and 6c, respectively, whereas the height profiles of two marked nanodroplets are given in Fig. 6d. These AFM photomicrographs clearly showed the formation of spherical nanosized homogenous droplets, with the mean diameters compatible with those determined by PCS and LD. Most importantly, no presence of larger droplets, aggregates or undissolved drug crystals was detected in the investigated nanoemulsion samples.

3.6. *In vivo* pharmacokinetic study

In order to evaluate the potential of the developed nanoemulsion carriers to deliver the model drug to the brain through the parenteral route, and to shed light on the specific role of nanoemulsion surface properties in brain drug targeting, the *in vivo* pharmacokinetic studies were performed in rats. Besides three selected RSP-loaded nanoemulsions (RSP-P80Sh, RSP-PL188Sh, and RSP-SHS15Sh), stabilized by lecithin in combination with P80, PL188, and SHS15 as co-emulsifiers, respectively, the co-emulsifier-free nanoemulsion formulation containing 2% (w/w) of lecithin, loaded with RSP (1 mg/g), was also prepared to assess the influence of the used co-emulsifier on the RSP pharmacokinetics. The physicochemical characteristics and stability data of this control nanoemulsion, RSP-LS75Sh, are described in Table S2 (Supplementary material). RSP content in all tested nanoemulsions was determined spectrophotometrically using corresponding blank, and the values were 100.7 ± 3.9, 100.1 ± 2.2, 100.7 ± 1.8, and 100.8 ± 2.9% for RSP-P80Sh, RSP-PL188Sh, RSP-SHS15Sh, and RSP-LS75Sh, respectively.

The concentration–time profiles of RSP in rat plasma and brain after i.p. administration of selected RSP nanoemulsions and RSP solution, along with their brain-to-plasma concentration ratios, are presented in Fig. 7, and the calculated pharmacokinetic parameters are summarized in Table 2. As the graphs show (Fig. 7), the mean plasma concentrations of RSP tended to be higher with nanoemulsions than with solution at the later time points (1–3 h post-injection), or in the case of RSP-P80Sh at all time points, with significant difference ($F_{(4,10)}$ = 10.977, p = 0.001) observed at 3 h post-injection for RSP-P80Sh, RSP-PL188Sh, and RSP-SHS15Sh nanoemulsions compared to control RSP solution. The possible explanation may be the formation of RSP depot at the i.p. injection site after administration of nanoemulsions, as well as slow release of incorporated RSP from the nanoemulsion oil

core into the blood, since the loaded drug needs time to transfer from the oil phase to the aqueous phase of nanoemulsion (Chen et al., 2010; Lu et al., 2009).

In addition, the mean plasma RSP concentrations after i.p. injection of nanoemulsions RSP-P80Sh, RSP-PL188Sh, and RSP-SHS15Sh were higher than those after control nanoemulsion formulation RSP-LS75Sh at most of time points (significant at 20 min ($F_{(4,10)}$ = 16.788, $p < 0.001$) and 180 min ($F_{(4,10)}$ = 10.977, p = 0.001) post-injection for RSP-P80Sh *vs.* RSP-LS75Sh and RSP-PL188Sh *vs.* RSP-LS75Sh), probably due to the smaller size of RSP-P80Sh, RSP-PL188Sh, and RSP-SHS15Sh nanoemulsion droplets coated with more hydrophilic surfactant film (due to the presence of co-emulsifier) compared to RSP-LS75Sh formulation, resulting in their prolonged retention in circulation and greater avoidance of the RES.

Although no significant differences were found in any of the studied plasma pharmacokinetic parameters (C_{max}, T_{max}, $AUC_{0–t}$, CL, $t_{1/2}$) of RSP from various vehicles, some trends could be recognized. For example, after i.p. injection, all nanoemulsions as well as solution showed similar mean plasma C_{max} values of RSP which were reached within 5–20 min, suggesting relatively rapid absorption into systemic circulation and subsequent fast distribution into the brain, with exception of nanoemulsions RSP-P80Sh and RSP-PL188Sh, both of which took longer but variable time (10-180 min, from a set to a set) to achieve the peak RSP concentrations in the brain. Furthermore, the mean plasma $AUC_{0–3\ h}$ tended to be higher when RSP was administered in the tested nanoemulsions compared to both control nanoemulsion RSP-LS75Sh and RSP solution, thus indicating an increased availability of RSP from nanoemulsions containing P80, PL188 or SHS15 as co-emulsifiers. Based on mean $AUC_{0–3\ h}$ values, relative bioavailability (F_{rel}) as well as absolute bioavailablity (F_{abs}) of RSP in plasma, the investigated nanoemulsions could be ranked in the following order: RSP-PL188Sh > RSP-P80Sh > RSP-SHS15Sh > RSP-LS75Sh.

The data obtained for brain tissue showed that there were high inter-individual variations of RSP concentrations at various time points, which could have masked apparent differences between tested RSP formulations. Significant difference ($F_{(4,10)}$ = 6.241, p = 0.009) was detected only for RSP-P80Sh nanoemulsion which produced higher mean brain RSP concentrations than RSP-SHS15Sh and RSP-LS75Sh formulations and RSP solution at 40 min post-injection. A tendency of increased brain concentrations of RSP formulated in RSP-P80Sh and RSP-PL188Sh nanoemulsions at the last time point (3 h after the dose), which in both cases was true for two of three sets of data, suggests that there might have been a time-consuming process such as, inter alia, receptor-mediated endocytosis/transcytosis, which promoted increased RSP uptake from these nanoemulsions into brain with time. As proposed by Kreuter (2001) for delivery of nanoparticles into brain, nanoemulsion droplets could have entered the brain by adsorption on brain capillary walls combined with increased retention in brain capillaries, creating higher concentration gradient which would enhance the transport across the brain capillary endothelial cells. Nanoemulsion droplets covered by combined lecithin/P80 or lecithin/PL188 emulsifier film could have also been uptaken into brain through endocytosis and/or transcytosis enabled by plasma apolipoproteins anchored on the droplet surface (Kreuter, 2001; Wohlfart et al., 2012; Kasongo et al., 2011). Finally, inhibition of P-glycoprotein efflux system at the BBB by P80 (Kreuter, 2001; Prabhakar et al., 2013) and probably by PL188 (Kabanov et al., 2003; Wohlfart et al., 2012) could have added to the tendency of improvement of RSP brain levels from P80- and PL188-containing nanoemulsions.

As an index of brain drug targeting, the brain-to-plasma concentration ratio of RSP from various formulations was calculated at each time point (Fig. 7). It was evident that mean RSP concentrations in plasma following i.p. administration of RSP nanoemulsions or RSP solution exceeded those in brain at most of time points, which is not surprising taking into account

relatively low lipophilicity of RSP (log *P* 3.04) as well as its efflux by P-glycoprotein expressed at the BBB (Aravagiri and Marder, 2002; Bundgaard et al., 2012). Nevertheless, the fact that brain-to-plasma concentration ratio of RSP tended to be > 1 when it was administered in nanoemulsions RSP-LS75Sh (at 1 h) and RSP-P80Sh or RSP-PL188Sh (3 h post-injection) could indicate the potential of these nanoemulsion carriers for RSP targeting to the brain.

There were no significant differences in either of brain pharmacokinetic parameters (C_{max}, T_{max}, AUC_{0-t}) calculated for four RSP nanoemulsions and RSP solution. Nevertheless, it is important to note that among the nanoemulsions the highest mean brain $AUC_{0-3\ h}$ was seen with the formulation RSP-P80Sh, followed by the RSP-LS75Sh and RSP-PL188Sh, and finally by the RSP-SHS15Sh nanoemulsion (Table 2). Since all nanoemulsion types were very similar regarding their measured physicochemical parameters – Z-Ave, PDI, and ZP (Table S2, Supplementary material), this trend could be ascribed primarily to the differences in the specific surface properties caused by the presence of co-emulsifiers with different structures, especially polyoxyethylene chains length, and consequently behavior at the oil–water interface. These findings suggest that neither droplet size, nor surface charge, but particle surface, i.e., the interfacial composition of the stabilizing layer, was the crucial factor responsible for BBB passage and differences in pharmacokinetic profiles of RSP.

In general, the total brain levels ($AUC_{0-3\ h,\ brain}$) of RSP were lower than those found in plasma ($AUC_{0-3\ h,\ plasma}$), which resulted in an overall brain-to-plasma exposure ratio, that is, brain-to-plasma partition coefficient (K_p), < 1 (Table 2). Although the co-emulsifier-free nanoemulsion (RSP-LS75Sh) tended to have the greatest K_p value, it could not be stated that this nanoemulsion delivered RSP to the brain significantly better than other formulations. Accordingly, the therapeutic availability, also referred to as relative uptake rate (R), was another parameter taken into account. As evidenced by the R values shown in Table 2, the

brain availability of RSP following nanoemulsion administration, excepting RSP-SHS15Sh, was enhanced compared to the i.p. solution. The higher brain uptake might have resulted from the simple diffusion through the BBB of free RSP released from nanoemulsion and endocytosis/transcytosis of RSP-loaded nanoemulsion droplets. Furthermore, the mean $AUC_{0–3\ h}$ in the brain of RSP-P80Sh nanoemulsion was 2-fold higher than for RSP solution and 1.4–7.4-fold higher than for other tested nanoemulsions, indicating that P80 might be a promising surfactant for enhancing RSP brain delivery. Although the developed nanoemulsions showed certain capability to target the brain, further experiments are needed to elucidate their *in vivo* fate and effect on RSP pharmacodynamics.

4. Conclusions

In this work, a systematic design of experiments approach was successfully applied to better understand the formulation and preparation of nanoemulsions as potential carriers for brain drug targeting. The results of performed general factorial design showed significant individual as well as mutual effect of tested formulation and process factors (co-emulsifier type, aqueous phase type, HPH method) affecting critical quality attributes (droplet size, PDI, ZP) of nanoemulsions. Based on physicochemical properties and stability during 4 months of storage at 25 °C and after autoclaving, the most suitable nanoemulsion formulations typically containing sodium oleate in aqueous phase and P80, PL188 or SHS15 as co-emulsifier were selected, loaded with RSP as a model drug, and prepared by hot HPH method. AFM corroborated the size measurement results, demonstrating uniform distribution of spherical droplets with the mean diameter below 200 nm, whereas DSC and FTIR analyses indicated that RSP was molecularly dispersed in the investigated nanoemulsions, without chemical interactions with other ingredients.

In vivo pharmacokinetic study demonstrated different brain profiles of RSP after i.p. administration of selected nanoemulsions costabilized with different co-emulsifiers, suggesting that nanoemulsion droplet surface, i.e., composition of the stabilizing film, was probably the key factor determining the BBB passage of RSP. From the targeting point of view, it could be deduced that among the tested nanoemulsions, the P80-costabilized one could be preferable for RSP delivery to the brain. However, additional investigations are necessary to validate the observed potential of developed nanoemulsions for improving RSP brain targeting after parenteral administration and to determine whether these findings may have clinical relevance and significant influence on RSP therapeutic efficacy.

Acknowledgments

This work was supported financially by the Ministry of Education, Science and Technological Development, Republic of Serbia, within the framework of the Projects TR34031, OI175076, and TR32008. The authors are grateful to Lipoid GmbH for supplying Lipoid Purified Soybean Oil 700, Lipoid S 75 and Lipoid Sodium Oleate B as well as to BASF SE for gifting Kolliphor® P 188 and Kolliphor® HS 15. The authors also would like to thank Mr Klaus Weyhing, Department of Pharmaceutical Technology at University of Tuebingen, for his experimental assistance.

References

Aravagiri, M., Marder, S.R., 2002. Brain, plasma and tissue pharmacokinetics of risperidone and 9-hydroxyrisperidone after separate oral administration to rats. Psychopharmacology 159, 424–431.

Batrakova, E.V., Kabanov, A.V., 2008. Pluronic block copolymers: evolution of drug delivery concept from inert nanocarriers to biological response modifiers. J. Control. Release 130, 98–106.

Benita, S., Levy MY. 1993. Submicron emulsions as colloidal drug carriers for intravenous administration: comprehensive physicochemical characterization. J. Pharm. Sci. 82, 1069–1079.

Blasi, P., Schoubben, A., Traina, G., Manfroni, G., Barberini, L., Alberti, P.F., Cirotto, C., Ricci, M., 2013. Lipid nanoparticles for brain targeting III. Long-term stability and in vivo toxicity. Int. J. Pharm. 454, 316–323.

Bundgaard, C., Jensen, C.J., Garmer, M., 2012. Species comparison of in vivo P-glycoprotein-mediated brain efflux using mdr1a-deficient rats and mice. Drug Metab. Dispos. 40, 461–466.

Chen, H., Shi, S., Zhao, M., Zhang, L., He, H., Tang, X., 2010. A lyophilized etoposide submicron emulsion with a high drug loading for intravenous injection: preparation, evaluation, and pharmacokinetics in rats. Drug Dev. Ind. Pharm. 36, 1444–1453.

Constantinides, P.P., Chaubal, M.V., Shorr, R., 2008. Advances in lipid nanodispersions for parenteral drug delivery and targeting. Adv. Drug Deliv. Rev. 17, 757–767.

Dhawan, S., Kapil, R., Singh, B., 2011. Formulation development and systematic optimization of solid lipid nanoparticles of quercetin for improved brain delivery. J. Pharm. Pharmacol. 63, 342–351.

D'Souza, S., Faraj, J., DeLuca, P., 2013. Microsphere delivery of Risperidone as an alternative to combination therapy. Eur. J. Pharm. Biopharm. 85, 613–619.

Driscoll, D.F., Bacon, M.N., Bistrian, B.R., 2000. Physicochemical stability of two different types of intravenous lipid emulsion as total nutrient admixtures. J. Parenter. Enteral Nutr. 24, 15–22.

Đorđević, S.M., Radulović, T.S., Cekić, N.D., Ranđelović, D.V., Savić, M.M., Krajišnik, D.R., Milić, J.R., Savić, S.D., 2013. Experimental design in formulation of diazepam nanoemulsions: physicochemical and pharmacokinetic performances. J. Pharm. Sci. 102, 4159–4172.

Floury, J., Desrumaux, A., Lardières, J., 2000. Effect of high-pressure homogenization on droplet size distributions and rheological properties of model oil-in-water emulsions. Innov. Food Sci. Emerg. Technol. 127–134.

Hanefeld, A., Schmidt, M., Geissler, S., Langguth, P., 2012. Lyophilized nanoemulsion. Patent US8211948 B2.

Jumaa, M., Müller, B.W., 2002. Parenteral emulsions stabilized with a mixture of phospholipids and PEG-660–12-hydroxy-stearate: evaluation of accelerated and long-term stability. Eur. J. Pharm. Biopharm. 54, 207–212.

Kabanov, A.V., Batrakova, E.V., Miller, D.W., 2003. Pluronic block copolymers as modulators of drug efflux transporter activity in the blood–brain barrier. Adv. Drug Deliv. Rev. 55, 151–164.

Kasongo, K.W., Jansch, M., Müller, R.H., Walker, R.B., 2011. Evaluation of the in vitro differential protein adsorption patterns of didanosine-loaded nanostructured lipid carriers (NLCs) for potential targeting to the brain. J. Liposome Res. 21, 245–254.

Keck, C.M., Jansch, M., Müller, R.H., 2013. Protein adsorption patterns and analysis on iv nanoemulsions-the key factor determining the organ distribution. Pharmaceutics 5, 36–68.

Kelmann, R.G., Kuminek, G., Teixeira, H.F., Koester, L.S., 2007. Carbamazepine parenteral nanoemulsions prepared by spontaneous emulsification process. Int. J. Pharm. 342, 231–239.

Kreuter, J., 2001. Nanoparticulate systems for brain delivery of drugs. Adv. Drug Deliv. Rev. 47, 65–81.

Kreuter, J., 2005. Application of nanoparticles for the delivery of drugs to the brain. Int. Congr. Ser. 1277, 85–94.

Kumar, M., Misra, A., Babbar, A.K., Mishra, A.K., Mishra, P., Pathak, K., 2008. Intranasal nanoemulsion based brain targeting drug delivery system of risperidone. Int. J. Pharm. 358, 285–291.

Li, X., Du, L., Wang, C., Liu, Y., Mei, X., Jin, Y., 2011. Highly efficient and lowly toxic docetaxel nanoemulsions for intravenous injection to animals. Pharmazie 66, 479–483.

Lin, X., Yang, S., Gou, J., Zhao, M., Zhang, Y., Qi, N., He, H., Cai, C., Tang, X., Guo, P., 2012. A novel risperidone-loaded SAIB-PLGA mixture matrix depot with a reduced burst release: effects of solvents and PLGA on drug release behaviors in vitro/in vivo. J. Mater. Sci. Mater. Med. 23, 443–455.

Lu, Y., Zhang, Y., Yang, Z., Tang, X., 2009. Formulation of an intravenous emulsion loaded with a clarithromycin–phospholipid complex and its pharmacokinetics in rats. Int. J. Pharm. 366, 160-169.

Ma, W.C., Zhang, Q., Li, H., Larregieu, C.A., Zhang, N., Chu, T., Jin, H., Mao, S.J., 2013. Development of intravenous lipid emulsion of α-asarone with significantly improved safety and enhanced efficacy. Int. J. Pharm. 450, 21–30.

Madhusudhan, B., Rambhau, D., Apte, S.S., Gopinath, D., 2007. 1-O-alkylglycerol stabilized carbamazepine intravenous o/w nanoemulsions for drug targeting in mice. J Drug Target. 15, 154–161.

Martins, S., Tho, I., Souto, E., Ferreira, D., Brandl, M., 2012. Multivariate design for the evaluation of lipid and surfactant composition effect for optimisation of lipid nanoparticles. Eur. J. Pharm. Sci. 45, 613–623.

Marín-Quintero, D., Fernández-Campos, F., Calpena-Campmany, A.C., Montes-López, M.J., Clares-Naveros, B., Del Pozo-Carrascosa, A., 2013. Formulation design and optimization for the improvement of nystatin–loaded lipid intravenous emulsion. J. Pharm. Sci. 102, 4015–4023.

Muthu, M.S., Rawat, M.K., Mishra, A., Singh, S., 2009. PLGA nanoparticle formulations of risperidone: preparation and neuropharmacological evaluation. Nanomedicine 5, 323–333.

Müller, R.H., Göppert, T.M., 2007. Protein adsorption patterns on parenteral lipid formulations: key factor determining the in vivo fate, in: Wasan, K.M. (Ed.), Role of lipid excipients in modifying oral and parenteral drug delivery: basic principles and biological examples. John Wiley & Sons Inc., Hoboken, New Jersey, pp. 124–159.

Nordén, T.P., Siekmann, B., Lundquist, S., Malmsten, M., 2001. Physicochemical characterisation of a drug–containing phospholipid–stabilised o/w emulsion for intravenous administration. Eur. J. Pharm. Sci. 13, 393–401.

Ould-Ouali, L., Noppe, M., Langlois, X., Willems, B., Te Riele, P., Timmerman, P., Brewster, M.E., Ariën, A., Préat, V., 2005. Self-assembling PEG-p(CL-co-TMC) copolymers for oral delivery of poorly water-soluble drugs: a case study with risperidone. J. Control. Release 102, 657–668.

Prabhakar, K., Afzal, S.M., Surender, G., Kishan, V., 2013. Tween 80 containing lipid nanoemulsions for delivery of indinavir to brain. Acta Pharm. Sin. B 3, 345–353.

Rund, D.A., Ewing, J.D., Mitzel, K., Votolato, N., 2006. The use of intramuscular benzodiazepines and antipsychotic agents in the treatment of acute agitation or violence in the emergency department. J. Emerg. Med. 31, 317–324.

Shi, S., Chen, H., Cui, Y., Tang, X., 2009. Formulation, stability and degradation kinetics of intravenous cinnarizine lipid emulsion. Int. J. Pharm. 373, 147–155.

Shinde, R.L., Jindal, A.B., Devarajan, P.V., 2011. Microemulsions and nanoemulsions for targeted drug delivery to the brain. Curr. Nanosci. 7, 119–133.

Silva, A.C., Kumar, A., Wild, W., Ferreira, D., Santos, D., Forbes, B., 2012. Long-term stability, biocompatibility and oral delivery potential of risperidone-loaded solid lipid nanoparticles. Int. J. Pharm. 436, 798–805.

Verma, S., Lan, Y., Gokhale, R., Burgess, D.J., 2009. Quality by design approach to understand the process of nanosuspension preparation. Int. J. Pharm. 377, 185–198.

Voigt, N., Henrich-Noack, P., Kockentiedt, S., Hintz, W., Tomas, J., Sabel, B.A., 2014. Surfactants, not size or zeta-potential influence blood-brain barrier passage of polymeric nanoparticles. Eur. J. Pharm. Biopharm. 87, 19–29.

Werling, J., Graham, S., Owen, H., Nair, L., Gonyon, T., Carter, P.W., 2008. Physicochemical stability of phospholipid-dispersed suspensions of crystalline itraconazole. Eur. J. Pharm. Biopharm. 69, 1104–1113.

Wohlfart, S., Gelperina, S., Kreuter, J., 2012. Transport of drugs across the blood-brain barrier by nanoparticles. J. Control. Release 161, 264–273.

Wong, H.L., Wu, X.Y., Bendayan, R., 2012. Nanotechnological advances for the delivery of CNS therapeutics. Adv. Drug Deliv. Rev. 64, 686–700.

Figure captions

Figure 1. Pareto plots for mean droplet size – Z-Ave (a), polydispersity index (b), and zeta potential (c) of designed nanoemulsions, along with the coefficient values and *p* values for the studied variables – A: co-emulsifier type; B: aqueous phase type; C: HPH method.

Figure 2. Interaction graphs for the mean droplet size (Z-Ave) of designed nanoemulsions.

Figure 3. Interaction graphs for the polydispersity index (PDI) of designed nanoemulsions.

Figure 4. Interaction graphs for the zeta potential (ZP) of designed nanoemulsions.

Figure 5. DSC thermograms of pure RSP, RSP-loaded (RSP-P80Sh) and blank (P80Sh) nanoemulsion (a); FTIR spectra of pure RSP, soybean lecithin (LS75), MCT–soybean oil (MCT–SO) mixture, RSP-loaded (RSP-P80Sh) and unloaded (P80Sh) nanoemulsion (b).

Figure 6. AFM images of RSP-loaded nanoemulsion (RSP-P80Sh): error signal of 2 x 2 μm^2 area of the sample (a), 2D topography (b), 3D topography (c), and height profiles of two selected nanoemulsion droplets (d).

Figure 7. Plasma and brain pharmacokinetic profiles and brain-to-plasma concentration ratios of RSP after intraperitoneal administration of RSP nanoemulsions (RSP-P80Sh, RSP-PL188Sh, RSP-SHS15Sh, and RSP-LS75Sh) and RSP solution to rats (mean ± SEM, n = 3); *$p < 0.05$, compared to RSP-P80Sh, RSP-LS75Sh, and RSP solution (ANOVA, $F_{(4,10)} = 6.581$, $p = 0.007$); **$p < 0.05$, compared to RSP-P80Sh and RSP-SHS15Sh (Mann–Whitney U test); ***$p < 0.05$, compared to RSP-P80Sh, RSP-PL188Sh, and RSP-SHS15Sh nanoemulsions (Mann–Whitney U test).

Table 1.

General factorial design matrix.

		Variables					
		Co-emulsifier type (A)		Aqueous phase type (B)		HPH method (C)	
Run	Formulation code	Actual level	Coded level	Actual level	Coded level	Actual level	Coded level
1	P80Pc	P80	{1 0}	PBS	–1	Cold	–1
2	P80Ph					Hot	1
3	P80Sc			SOS	1	Cold	–1
4	P80Sh					Hot	1
5	PL188Pc	PL188	{0 1}	PBS	–1	Cold	–1
6	PL188Ph					Hot	1
7	PL188Sc			SOS	1	Cold	–1
8	PL188Sh					Hot	1
9	SHS15Pc	SHS15	{–1 –1}	PBS	–1	Cold	–1
10	SHS15Ph					Hot	1
11	SHS15Sc			SOS	1	Cold	–1
12	SHS15Sh					Hot	1

P80: polysorbate 80; PL188: poloxamer 188; SHS15: Solutol® HS 15; PBS: phosphate buffer solution; SOS: sodium oleate aqueous solution.

Table 2.

Pharmacokinetic parameters of risperidone after intraperitoneal administration of selected risperidone-loaded nanoemulsions and risperidone solution (free risperidone) to rats (mean ± SEM, n = 3).

Parameter		Formulation				
		RSP-P80Sh	RSP-PL188Sh	RSP-SHS15Sh	RSP-LS75Sh	RSP-solution
	Plasma					
C_{max} (ng/mL)		780.07 ± 127.55	781.00 ± 34.87	614.10 ± 48.34	573.96 ± 14.62	639.29 ± 82.04
T_{max} (h)		0.31 ± 0.18	0.19 ± 0.07	0.11 ± 0.03	0.14 ± 0.03	0.11 ± 0.03
AUC_{0-t} (h ng/mL)		567.83 ± 78.99	642.79 ± 75.97	366.29 ± 140.81	265.49 ± 26.94	268.96 ± 35.24
CL (L/h/kg)		1.82 ± 0.23	1.60 ± 0.19	3.48 ± 0.97	3.84 ± 0.37	3.84 ± 0.45
$T_{1/2}$ (h)		1.53 ± 0.51	0.87 ± 0.13	1.11 ± 0.25	0.73 ± 0.17	0.92 ± 0.21
F_{rel} (%)		211.12	238.99	136.19	98.71	–
F_{abs} (%)		77.21	87.40	49.81	36.10	36.57
	Brain					
C_{max} (ng/g)		292.96 ± 106.76	136.28 ± 48.16	170.87 ± 22.92	199.63 ± 43.54	158.09 ± 27.17
T_{max} (h)		1.17 ± 0.92	1.11 ± 0.94	0.08 ± 0.00	0.44 ± 0.28	0.11 ± 0.03
AUC_{0-t} (h ng/g)		277.06 ± 155.49	150.29 ± 101.36	37.25 ± 10.39	195.39 ± 96.81	135.57 ± 29.62
Kp		0.51 ± 0.32	0.28 ± 0.21	0.13 ± 0.05	0.81 ± 0.46	0.51 ± 0.13
DTI		1.00	0.54	0.25	1.57	–
R		2.04	1.11	0.27	1.44	–

Values are shown as means ± SEM (n = 3). DTI: drug targeting index ($Kp_{RSP\ nanoemulsion}/Kp_{RSP\ solution}$).

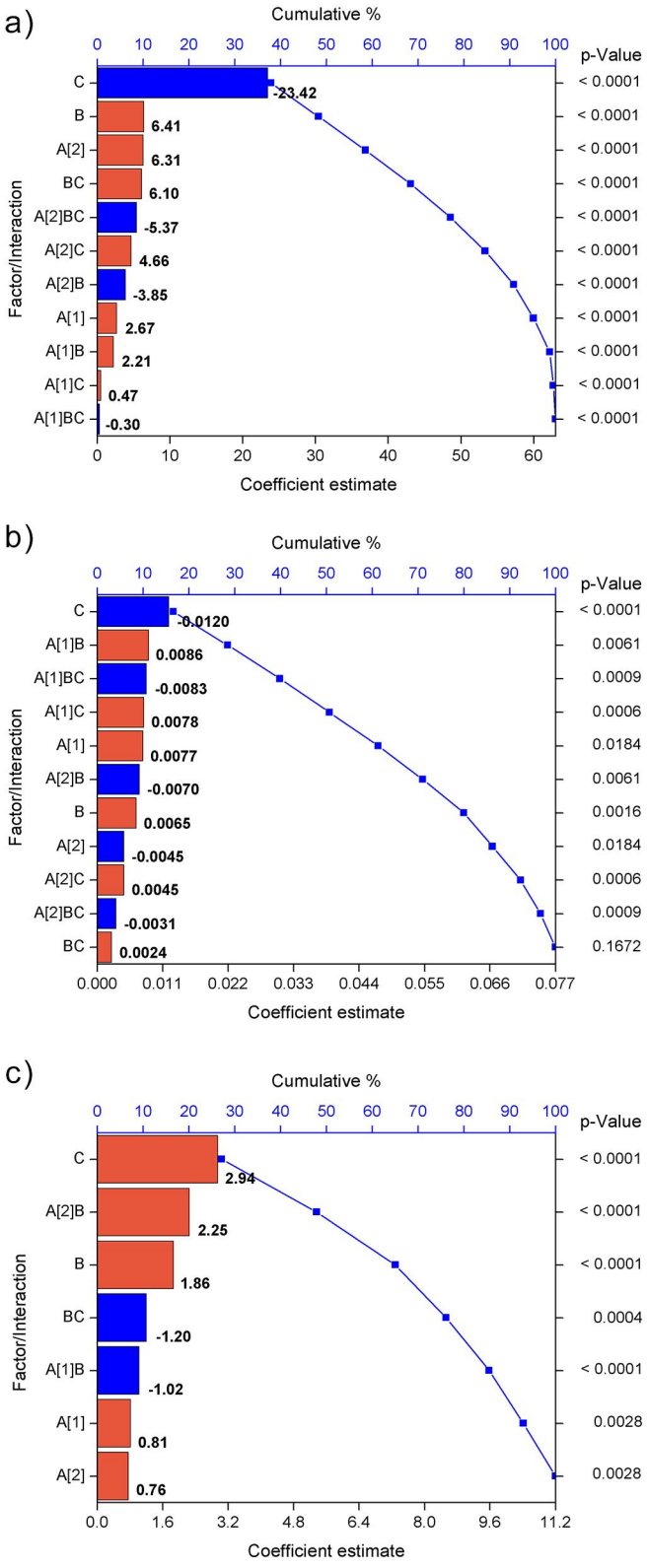

Fig. 1

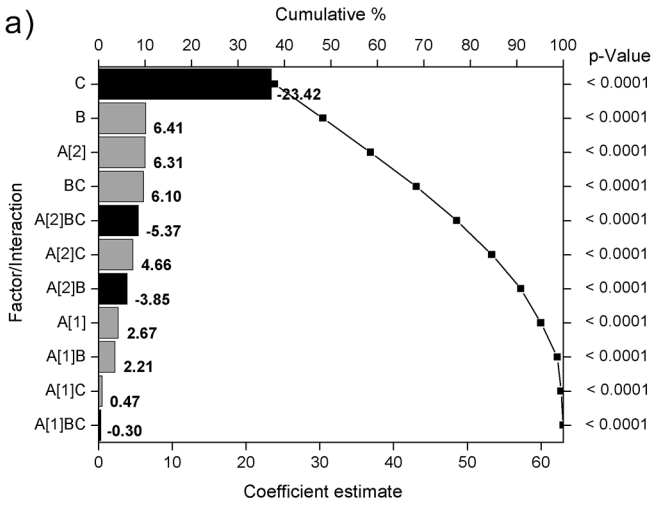

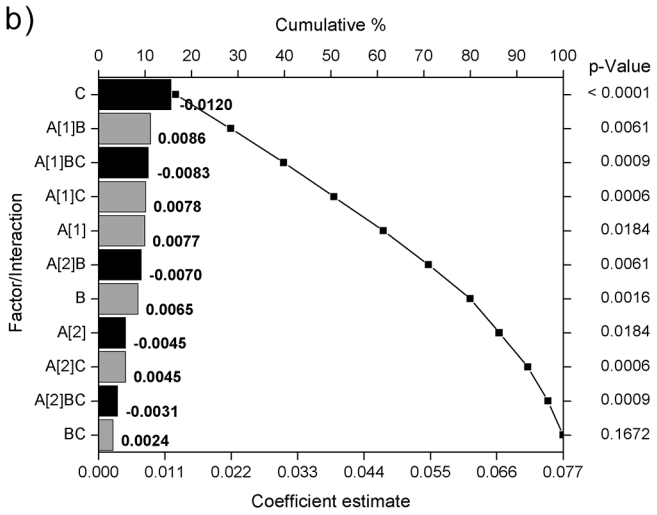

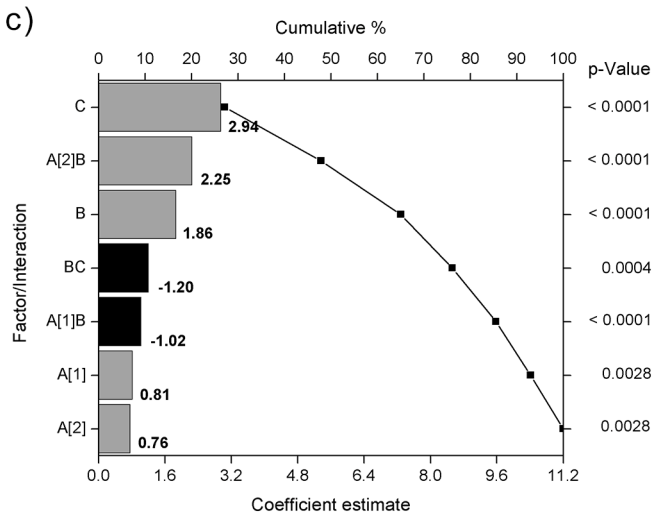

Fig. 1

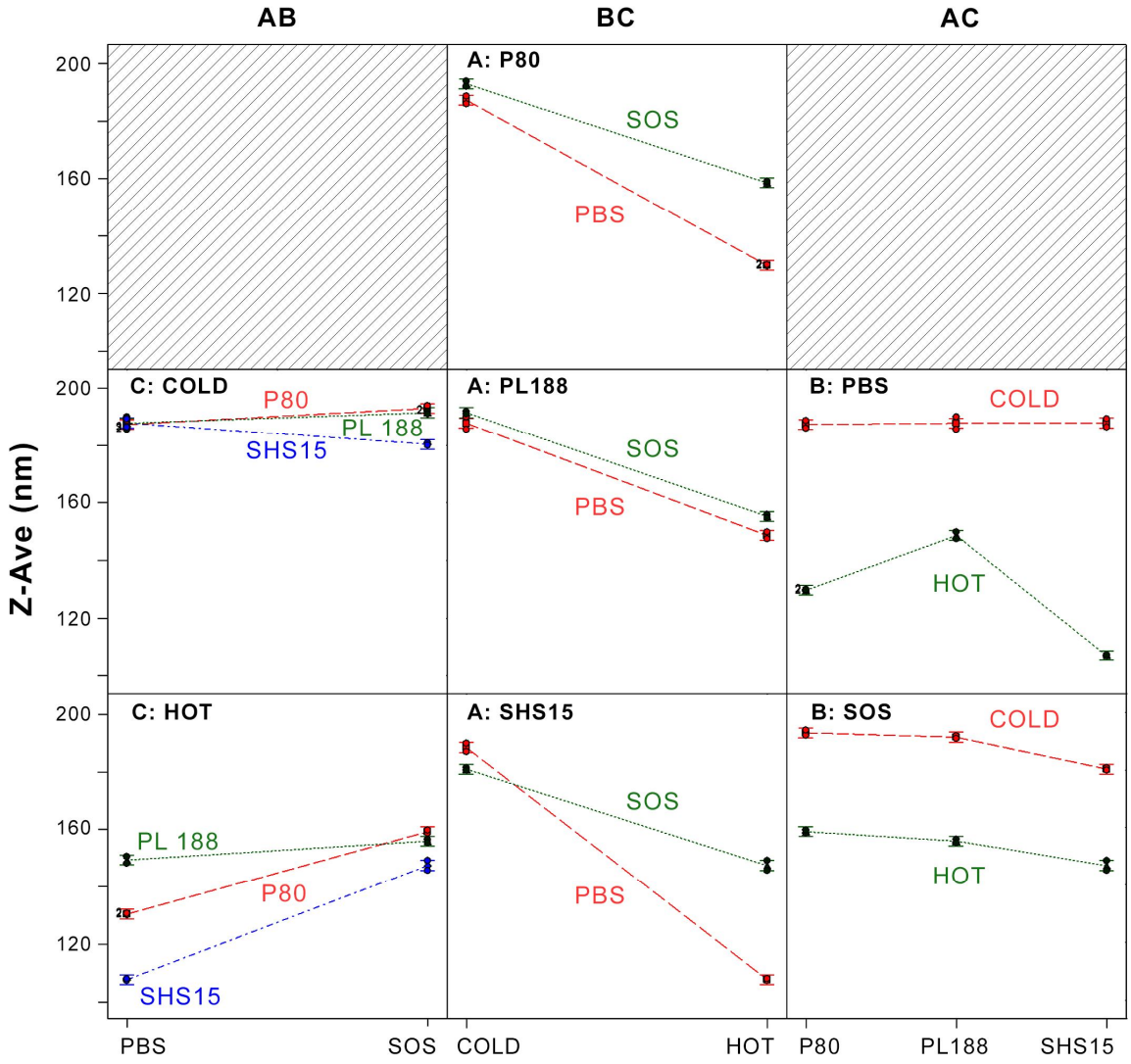

Fig.2

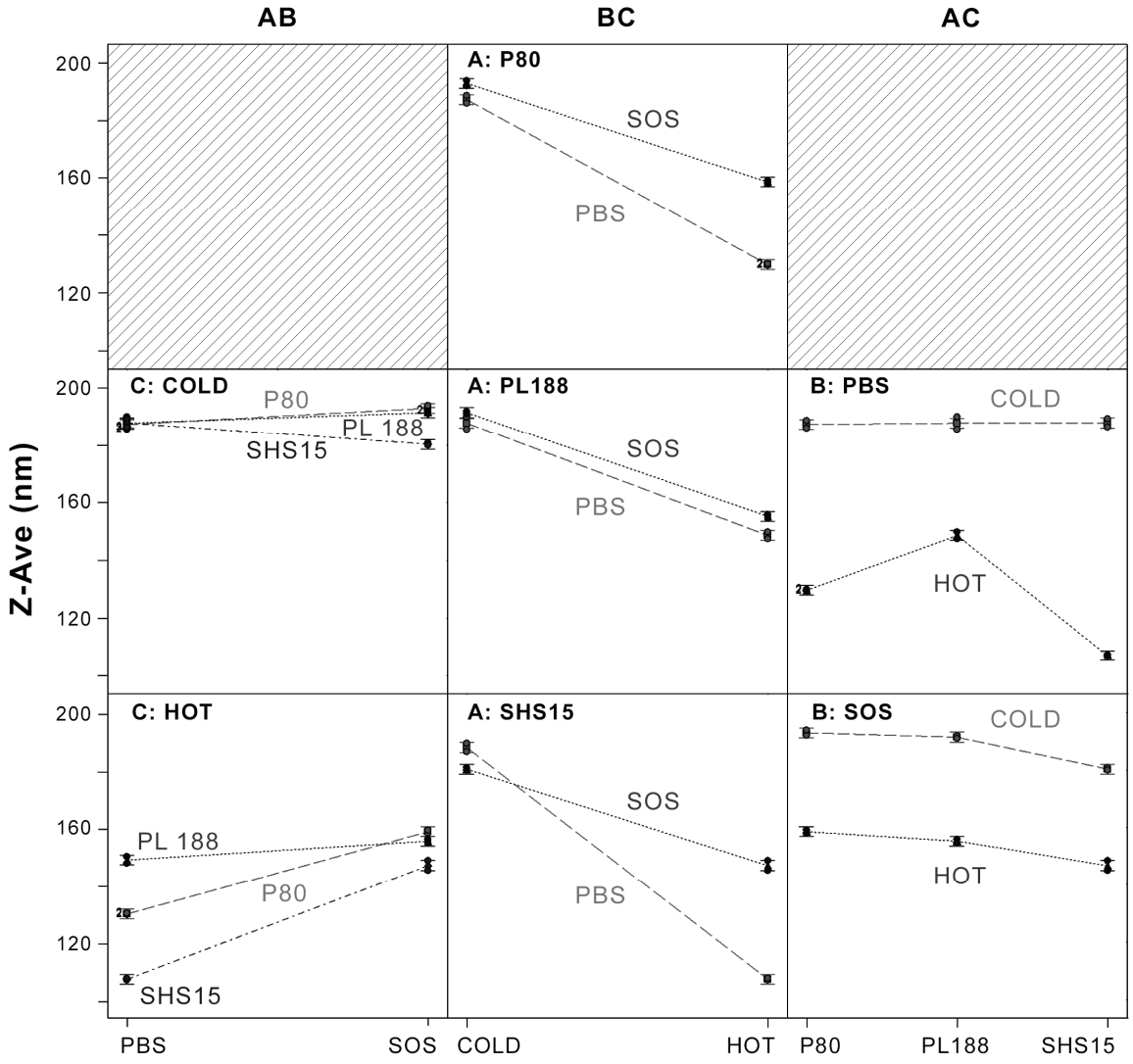

Fig.2

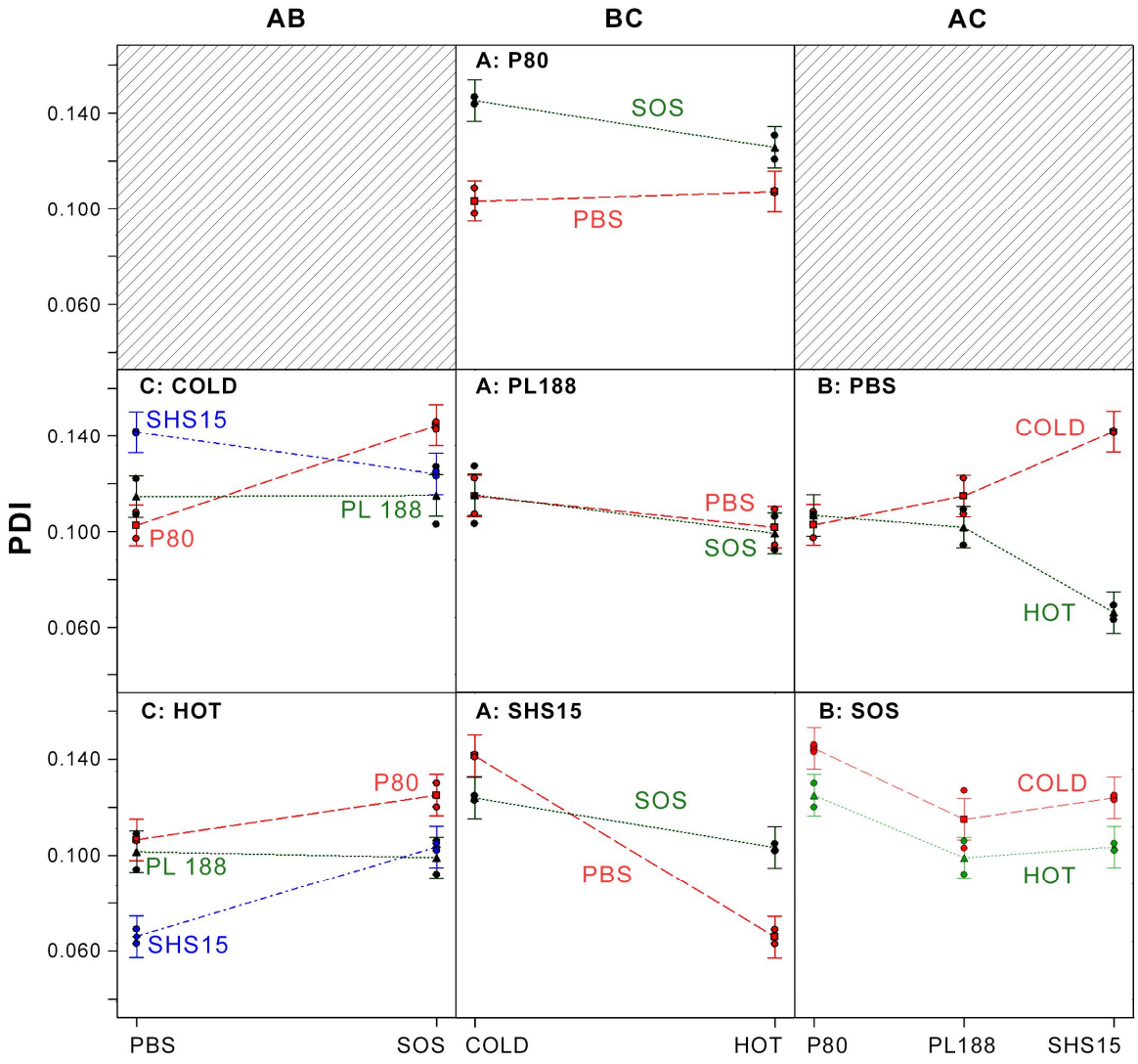

Fig. 3

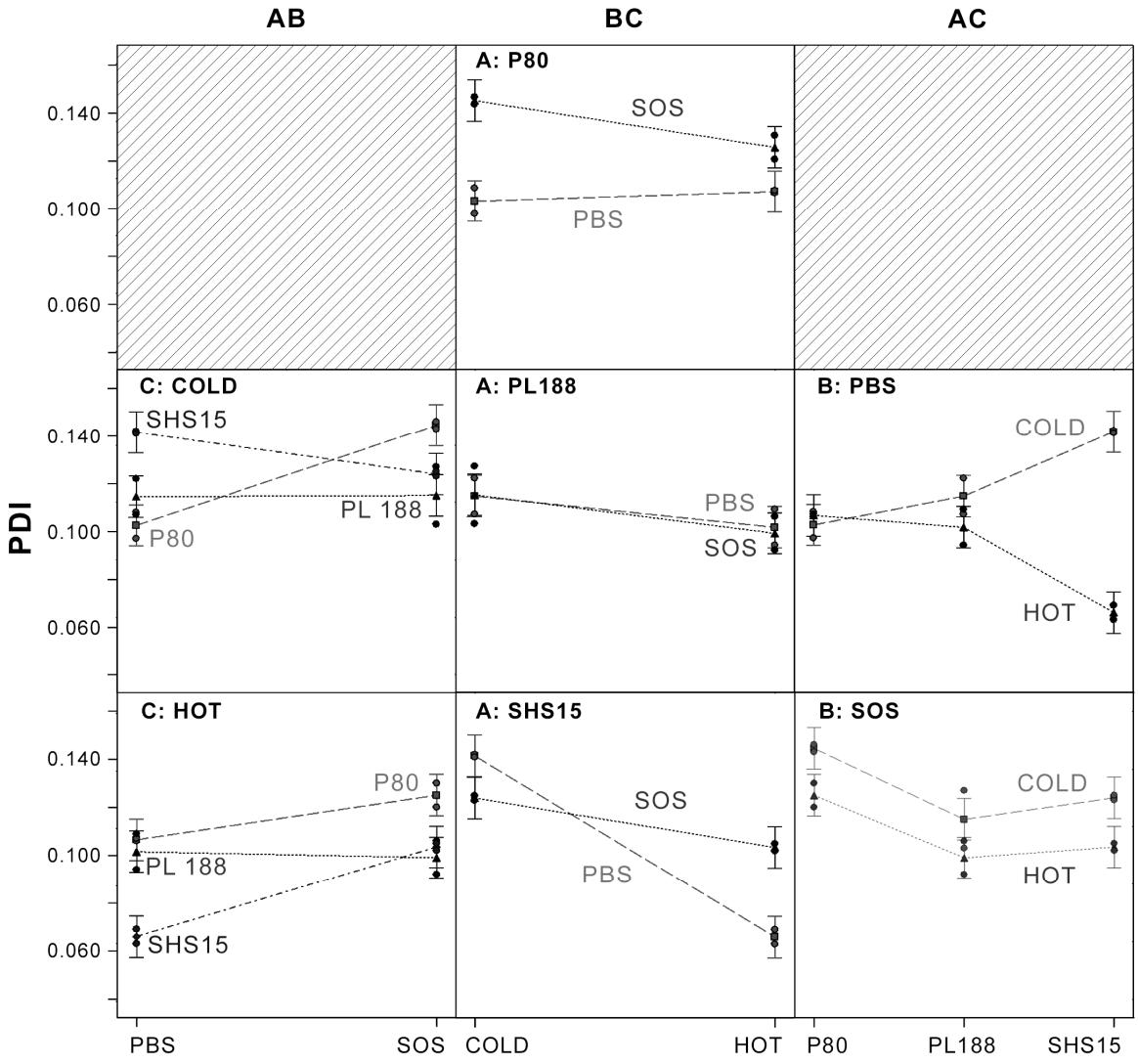

Fig. 3

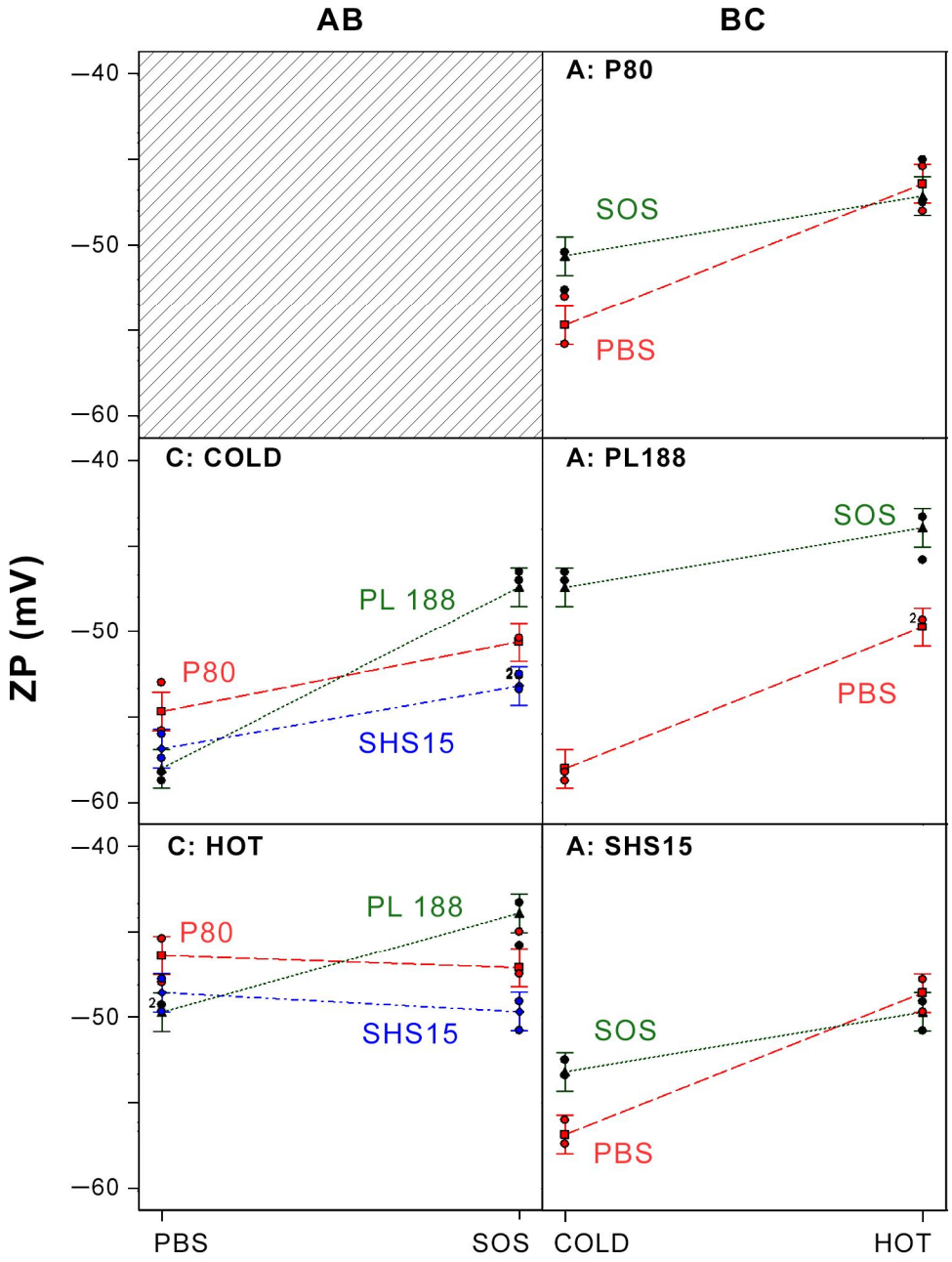

Fig. 4

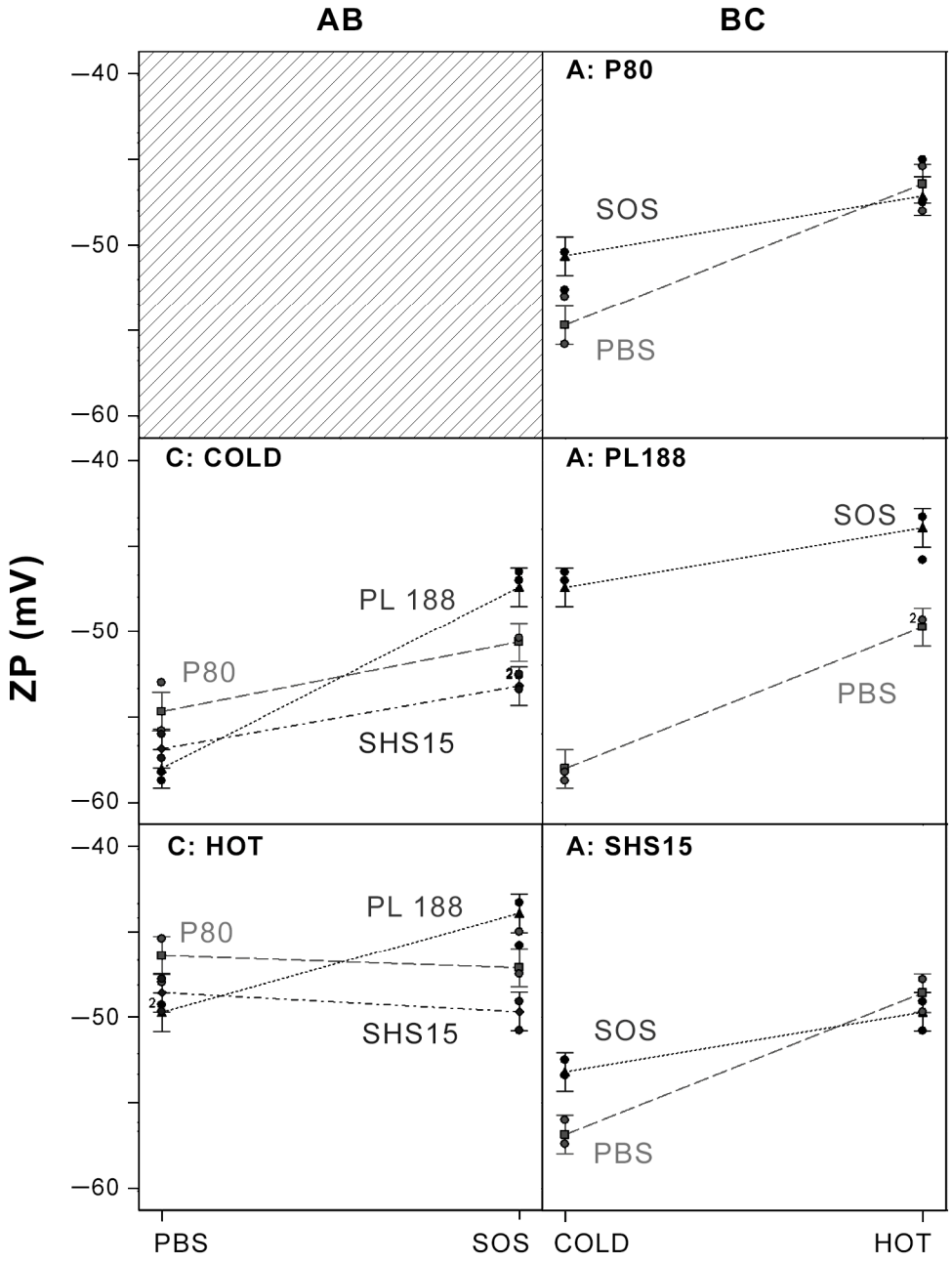

Fig. 4

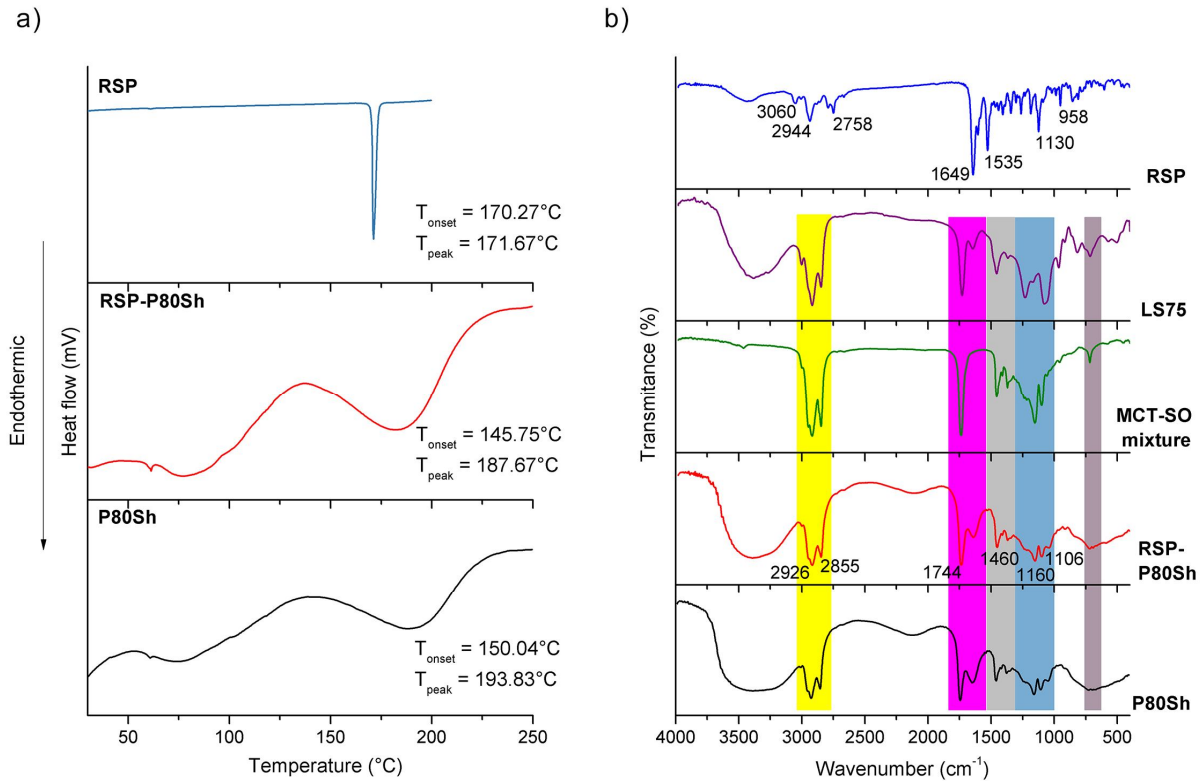

Fig. 5

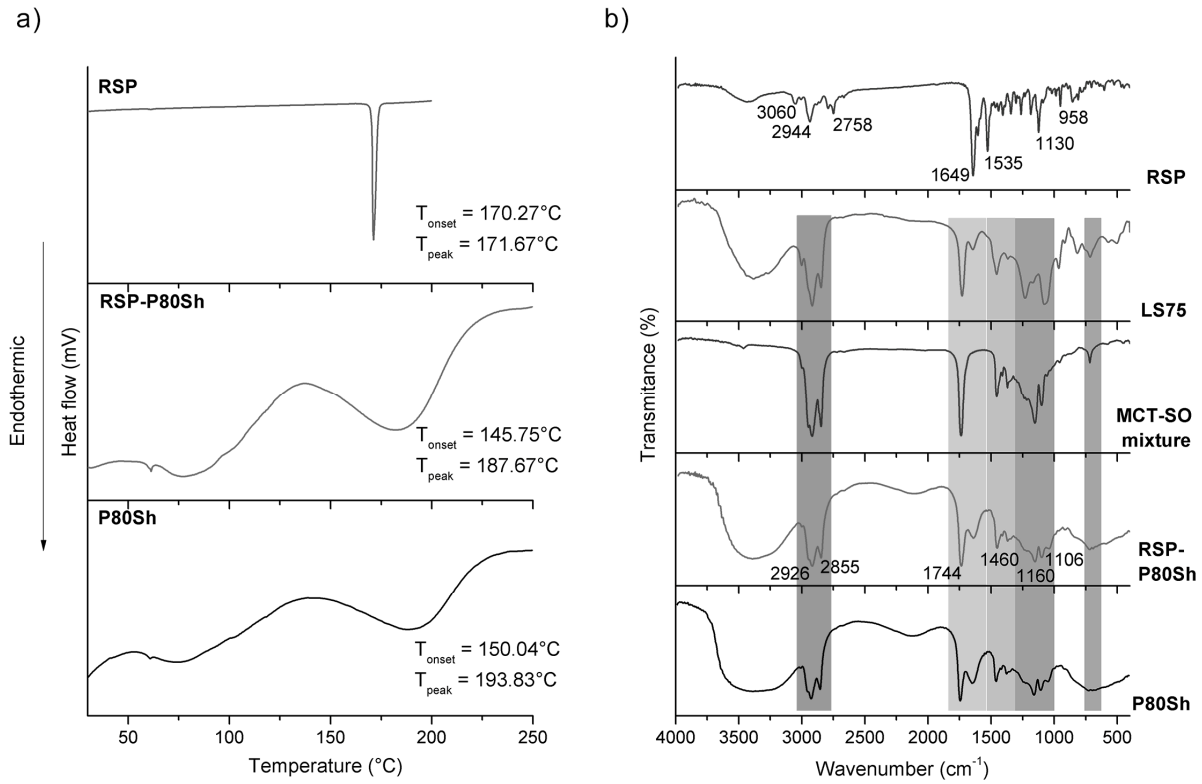

Fig. 5

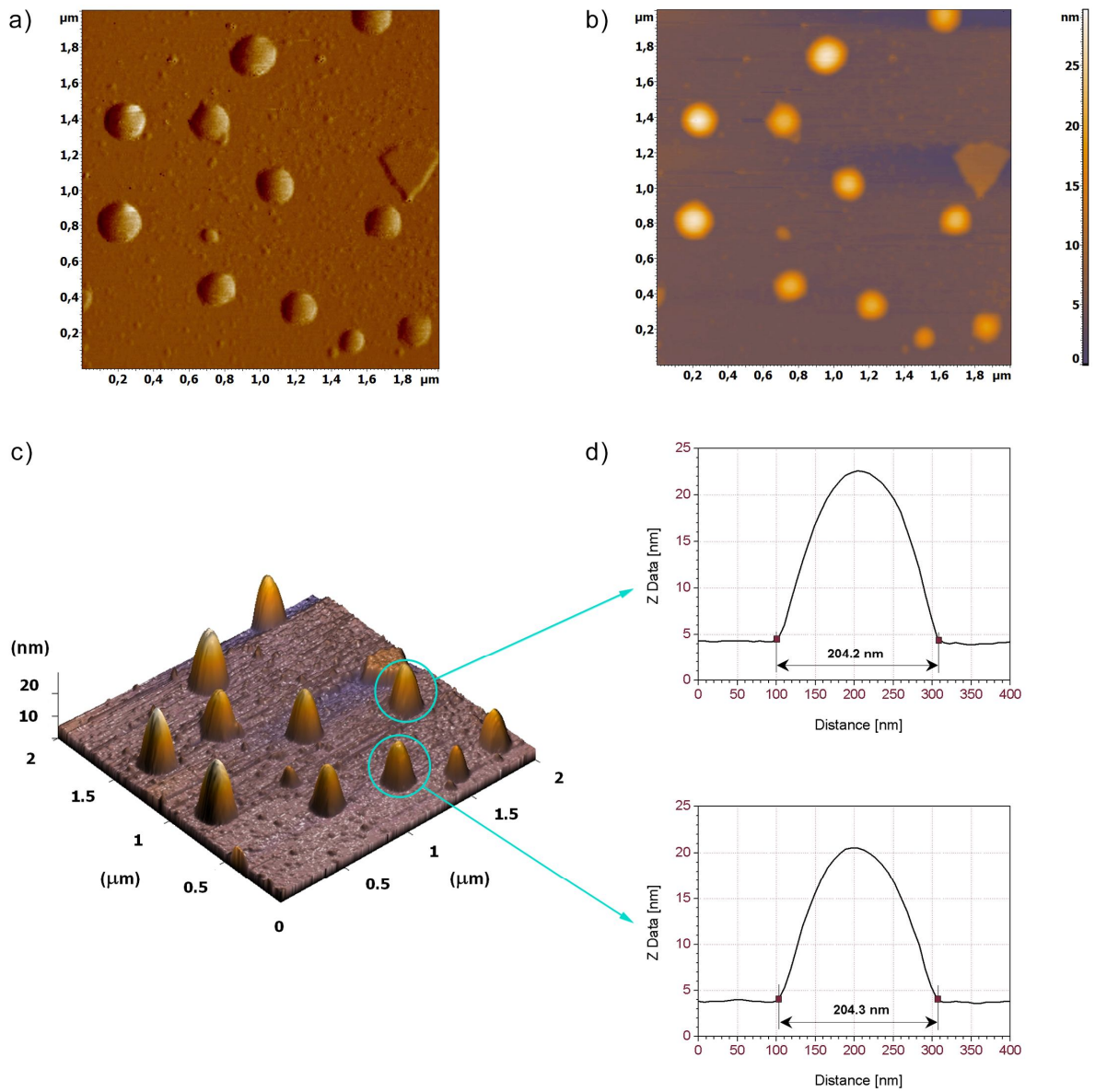

Fig. 6

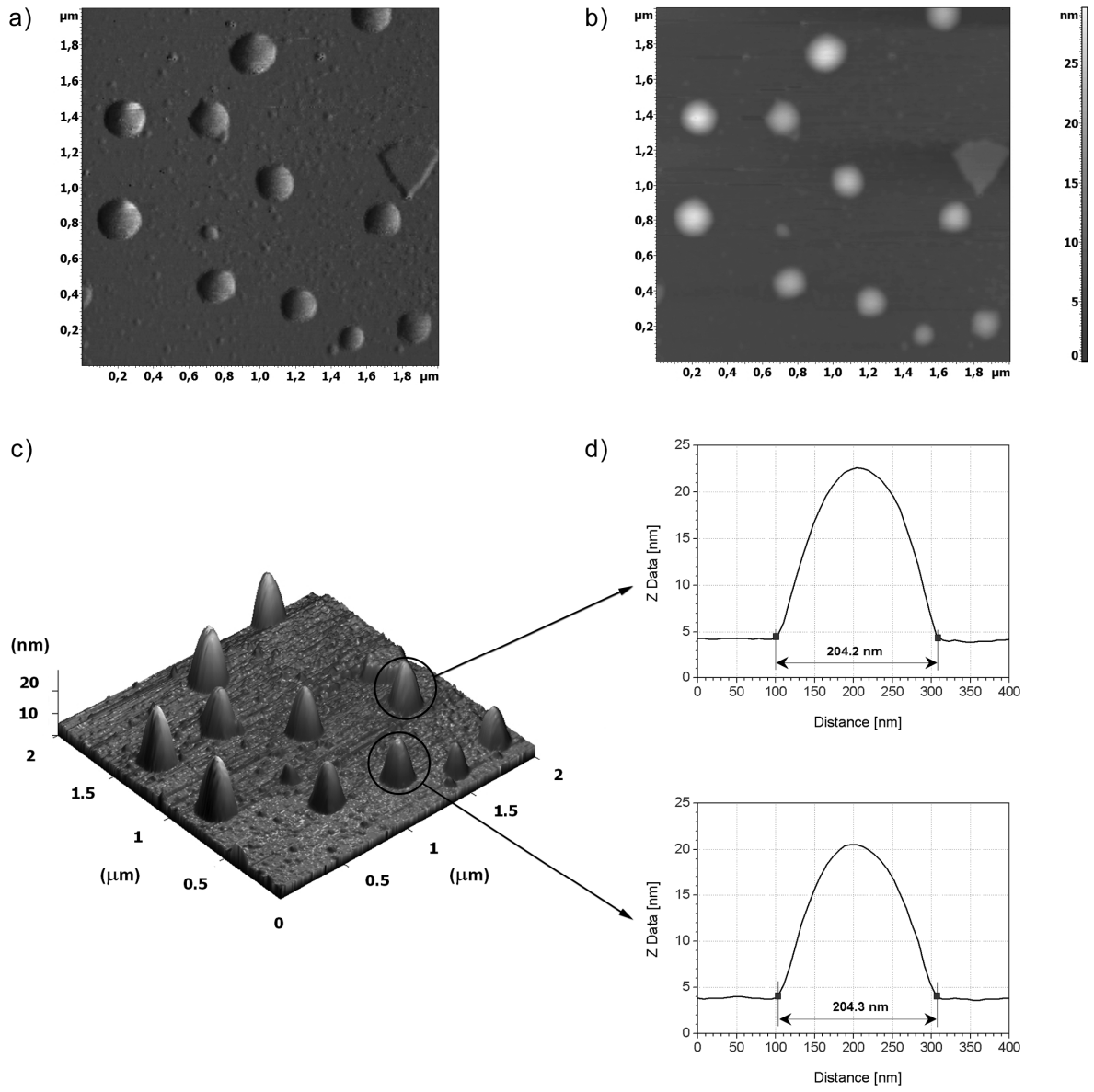

Fig. 6

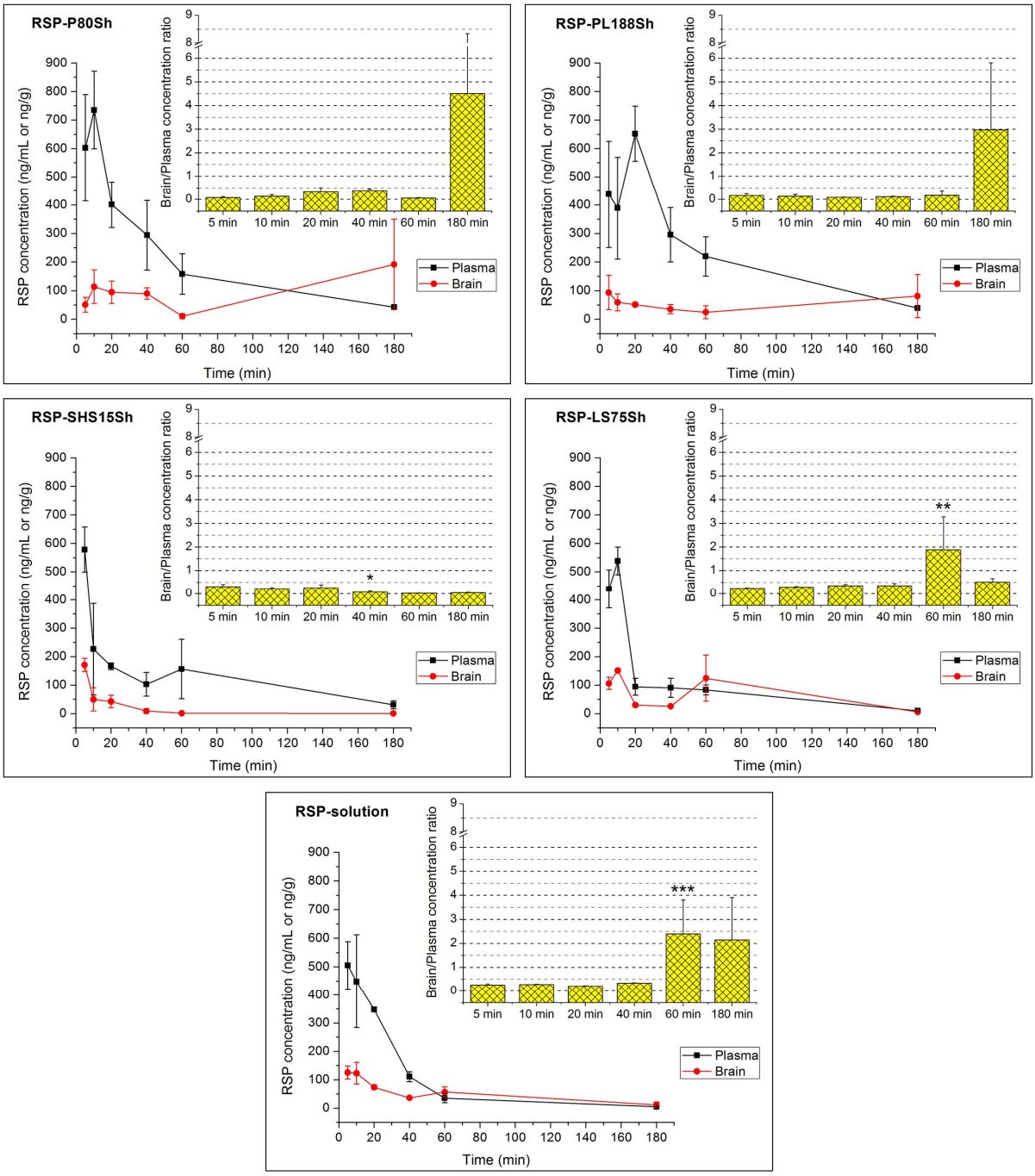

Fig. 7

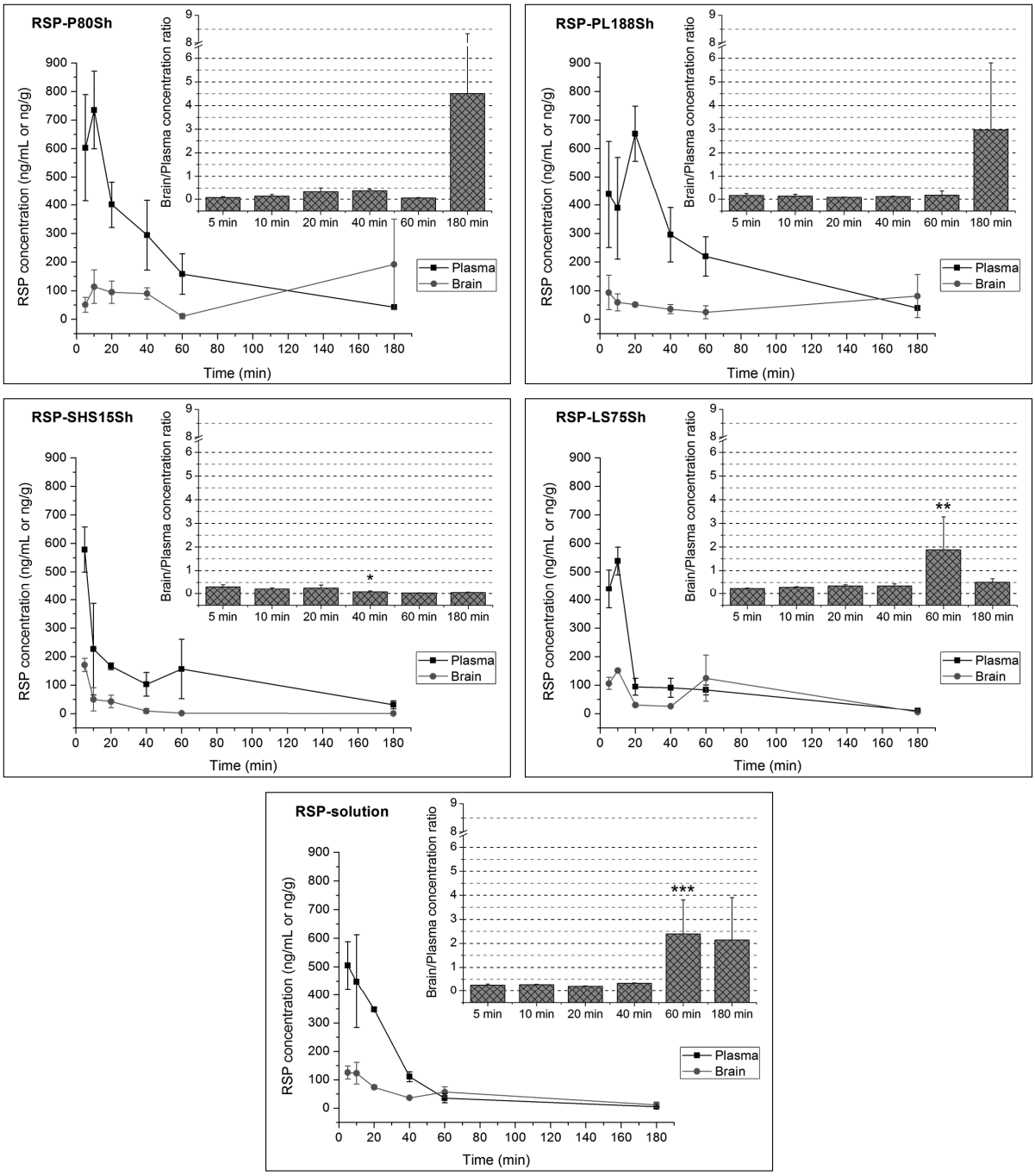

Fig. 7